INVESTIGATION OF ARTERIAL COMPLIANCE AND WAVE REFLECTIONS AS MARKERS OF HYPERTENSION

By

NIHIR BHAVSAR

A thesis submitted to the

Graduate School-New Brunswick

Rutgers, The State University of New Jersey

and

The Graduate School of Biomedical Science

UMDNJ – Robert Wood Johnson Medical School

in partial fulfillment of the requirements

for the Joint degree of

Master of Science

Graduate Program in Biomedical Engineering

written under the direction of

Professor John K-J. Li

and approved by

_____

_____

_____

New Brunswick, New Jersey

October, 2012

ABSTRACT OF THE THESIS

INVESTIGATION OF ARTERIAL COMPLIANCE AND WAVE REFLECTIONS AS MARKERS OF HYPERTENSION

By **NIHIR BHAVSAR**

Thesis Director

Professor John K-J. Li

Hypertension is the primary risk factor for many forms of cardiovascular diseases, which are the leading cause of death in the developed world. Hypertension and myocardial ischemia are also main contributors to stroke, which results in serious and long-term disability. Early detection, monitoring, and treatment of hypertension and myocardial ischemia are thus important in the delay or prevention of morbidity and mortality from cardiovascular diseases. This thesis investigates new hemodynamic markers that are critical in the diagnosis and assessment of the severity of hypertension and myocardial ischemia.

Experimental data was obtained from anesthetized mongrel dogs for control, hypertension, vasodilation, and myocardial ischemia. Simultaneously recorded aortic pressure and aortic flow waveforms were digitized for calculations of hemodynamic parameters. Model-based linear and nonlinear arterial compliances, the compliance-pressure relationship, and different augmentation indices for assessing the effects of wave reflections were computed and evaluated as markers of hypertension.

Analysis of the modified three-element nonlinear Windkessel model or the Li-Model revealed a nonlinear blood pressure and arterial compliance relationship and indicated that this model better predicts the blood pressure waveforms during hypertension and vasodilation. The compliance-pressure loops constructed for a single beat demonstrated reduced compliance during hypertension and increased compliance during vasodilation and ischemia. Analysis of the augmentation index revealed that blood pressure is indeed augmented in systole during hypertension and reduced during vasodilation and ischemia. The newly presented methods for augmentation index calculation are also shown to be better indicators of wave reflection effects in hypertension. Thus, these new nonlinear compliance and augmentation indices may be useful markers in the diagnosis and treatment of hypertension.

ACKNOWLEDGEMENT

Foremost, I would like to express my deepest gratitude to my advisor, Dr. John K-J. Li. This thesis could not have been completed without his guidance, knowledge, encouragement, and continuous support.

I would also like to thank my parents, Rashmikant and Bina Bhavsar, and my sister, Sona Bhavsar, for their love, advice, and unconditional support in all my endeavors.

TABLE OF CONTENTS

LIST OF TABLES

LIST OF ILLUSTRATIONS

Chapter 1: Introduction

1.1. Circulatory System Anatomy

The circulatory system includes the heart, the blood vessels, and blood. The heart acts as a muscular pump to push blood through the blood vessels by rhythmic contractions. The contractions generate enough pressure to create the necessary driving pressure for blood to flow to the tissues. The blood vessels act as passageways for blood to be distributed from the heart to organ vascular beds and then returned to the heart via veins. Blood transports materials such as oxygen and nutrients are transported throughout the body (Sherwood 2010).

1.1.1. Heart

The heart is composed of cardiac muscle and connective tissue. It has a wide base and a sharper apex. The heart is divided into two halves and four chambers. The right and left atria are the top two chambers and receive blood returning to the heart, while the right and left ventricles are the bottom two chambers and pump blood from the heart. The left side of the heart has oxygenated blood, while the right side has oxygen-deprived blood.

The right atrium receives deoxygenated blood from the superior and inferior vena cava. The deoxygenated blood flows through the tricuspid valve and into the right ventricle. From the right ventricle, the blood is pumped through the pulmonary valve and into the pulmonary artery. The pulmonary artery bifurcates and carries blood to the lungs to be oxygenated. The newly oxygenated blood is carried by the pulmonary veins back to

the left atrium. The blood travels to the left ventricle via the mitral valve and then into the aorta via the aortic valve. The blood is finally delivered to the body via the arterial tree.

The heart wall consists of three layers: the endothelium, myocardium, and epicardium. The endothelium is the innermost layer and is composed of a unique epithelial tissue. The myocardium is a middle layer composed of cardiac muscle and constitutes the majority of the heart wall. The epicardium is a thin outer layer that encases the heart. The cardiac muscle consists of two types of specialized cells. Contractile cells pump blood and encompass 99% of the cardiac muscle cells. Autorhythmic cells initiate and conduct the action potentials that stimulate contraction. Since heart muscle cells cannot divide, they have an abundance of mitochondria and receive a rich blood supply to support their lifelong contractile activity (Sherwood 2010).

1.1.2. Blood vessels

Blood vessels are responsible for transporting blood between the heart and body. The blood vessels are arranged in a vascular loop with a parallel arrangement of vessels branching off of the aorta to form the arterial tree. This arrangement allows for the blood to be distributed to the systemic organs in different proportions. Additionally, no organ receives blood that has already passed through another organ ensuring that all organs receive sufficiently oxygenated blood.

The vascular loop, beginning and ending at the heart, consists of various types of blood vessels. The aorta is the major artery of the body and carries blood directly from the left ventricle of the heart. Arteries branch from the aorta and continue to bifurcate into a tree-like network of progressively smaller arteries in order to deliver blood to the

different organs of the body. Once a small artery reaches an organ, it branches into smaller arterioles. Arterioles are considered primary resistance vessels since the body adjusts their diameter to control the amount of blood flow reaching each organ. Lastly, the arterioles branch into capillaries, which are the smallest blood vessels. Capillaries are responsible for the exchange of oxygen and nutrients with the surrounding cells. Following this site of exchange, the capillaries rejoin into small venules. These small venules combine into veins and exit the organs. The small veins combine into larger veins and return to the heart (Sherwood 2010).

The general structure of blood vessels consists of the tunica intima, tunica media, and tunica adventitia. The tunica intima is the innermost layer of the blood vessel wall and functions as the physical barrier to the blood. This layer consists of an endothelium comprised of a simple squamous epithelium. The tunica intima is differentiated from the tunica media by an internal elastic lamina (elastic tissue). The tunica media consists of smooth muscle cells and elastic tissue. This layer is the thickest part of the arterial wall, however is thin and indistinct in veins. The tunica media is differentiated from the tunica adventitia by an external elastic lamina. The elastic tissue present in these inner layers give blood vessels an elastic property. The elasticity maintains the pressure within the blood vessels to ensure forward blood flow during diastole. The tunica adventitia is the outermost layer of the blood vessel wall and is made of connective tissue and some smooth muscle. In veins, this layer is the thickest part of the vessel wall (Henrikson, et. al. 1997).

1.1.3. Humans versus dogs

The data presented in this thesis was obtained from experiments conducted on mongrel dogs. The dog's circulatory system is similar to humans. Their heart contains four chambers with the pulmonary side receiving deoxygenated blood and the systemic side sending oxygenated blood. Additionally, previous studies have demonstrated that dog's blood vessels are morphologically and histologically similar to their human counterparts (Sasajima, et. al. 1999). Physiologically, the cardiac electrical conduction system in dogs is also similar to humans (National Research Council 2009). The extensive similarities between the dog and human circulatory systems allow for the extrapolation of the data analysis to humans.

1.2. Cardiovascular Disease

Cardiovascular disease (CVD) is a class of diseases that includes atherosclerosis, coronary heart disease, stroke, myocardial ischemia, heart failure, and high blood pressure. These cardiac diseases have a variety of risk factors and together are one of the leading causes of death in United States (U.S.). Approximately one in every three adults has at least one type of cardiovascular disease. In 2006, cardiovascular disease was the underlying cause in 34.2% of all deaths in the U.S. Additionally, it was a contributing factor in 56% of all deaths (Lloyd-Jones, et. al. 2008).

1.2.1. Atherosclerosis

Atherosclerosis is a systemic disease process that leads to the hardening of arteries (arterial stiffness) due to fatty deposits, inflammation, scar tissue, and the build up of cells within the arterial walls. Atherosclerosis is considered an underlying cause in

the majority of clinical cardiovascular events. The main indicators are coronary artery calcification (CAC) and carotid intima media thickness (IMT). Coronary artery calcification measures the burden of atherosclerosis in the heart arteries. Carotid IMT measures the thickness of the tunica intima and tunica media of the carotid artery walls and is an early manifestation of the disease (Lloyd-Jones, et. al. 2008).

The major risk factors for atherosclerosis include hypertension, diabetes, smoking, and a family history of the disease. The prevention guidelines call for a healthy diet (specifically avoiding fatty foods), limited alcohol intake, and exercise (Bonow, et. al. 2011).

1.2.2. Coronary Heart Disease

Coronary heart disease (CHD) is the narrowing of the small blood to the heart and commonly leads to myocardial infarction (MI). Coronary heart disease is responsible for approximately 20% of all deaths in the U.S. A patient who has survived the acute stage of a myocardial infarction has a 1.5 to 15 times increased prevalence of illness and death. In addition, any patient at least forty years old who suffers a myocardial infarction has an 18-23% chance of death within one year and a 33-43% chance of death within five years. The major risk factors for CHD are hypertension, high blood cholesterol level, smoking, and diabetes (Lloyd-Jones, et. al. 2008). The various treatment regimens consist of administration of angiotensin-converting-enzyme (ACE) inhibitors (decrease blood pressure), aspirin (prevent blood clots) (Calonge, et. al. 2009), beta-blockers (decrease heart rate), or calcium channel blockers (relax the blood vessels) (Bonow, et. al. 2011).

1.2.3. Stroke

A stroke is when blood flow to any part of the brain is obstructed. Strokes are the third most common cause of death aside from only heart disease and cancer. It is also the most common cause of long-term disability in the U.S. Any patient at least forty years old who suffers a stroke has a 21-24% chance of death within 1 year and a 47-51% chance of death within five years. The major risk factors for stroke include hypertension, ischemia, and smoking (Lloyd-Jones, et. al. 2008). Stroke is considered a medical emergency and requires immediate hospitalization for treatment. The most common treatments involve the administration of blood thinners or surgery to break up the obstructing clot (Goldstein, et. al. 2011).

1.2.4. Myocardial Ischemia

An imbalance between oxygen supply and demand due to a restricted blood flow results in myocardial ischemia. The lack of oxygen and nutrients reduces the energy available to the cells, leading to cell and tissue damage. The extent of the injury is dependent on the severity (a partial or complete obstruction), duration, temporal sequence, and inflammatory response. Since ischemia leads directly to cell damage, the ability to monitor and detect occurrences is vital. The major causes of myocardial ischemia are atherosclerosis, blood clots, coronary spasm, and severe illness. The important risk factors include smoking, hypertension, and a lack of physical activity. (Cokkinos, et. al. 2006)

1.2.5. Hypertension (High Blood Pressure)

The American Heart Association categorizes a person as having normal blood pressure if their systolic and diastolic blood pressures are less than 120 mmHg and 80 mmHg, respectively. Hypertension is defined as a systolic or diastolic blood pressure greater than 139 mmHg or 89 mmHg, respectively. Table 1.1 shows a breakdown of the blood pressure categories. In 2006, 29% of U.S. adults were hypertensive and an additional 37% were prehypertensive. 22% of the hypertensive adults were unaware of their condition and were not taking prevention steps or receiving any treatment. As described in the previous sections, in addition to being it's own disease, hypertension is a major risk factor for many other cardiovascular diseases. Two-thirds of heart attack and stroke patients were hypertensive. (Lloyd-Jones, et. al. 2008). The prevention guidelines include a healthy diet, exercise, limited alcohol intake, limited sodium intake, and reduced stress. The main treatment is the administration of antihypertensive drugs (Bonow, et. al. 2011).

Blood Pressure Category	Systolic (mmHg)		Diastolic (mmHg)
Normal	< 120	and	< 80
Prehypertension	120 - 139	or	80 - 89
Hypertension Stage 1	140 - 159	or	90 - 99
Hypertension Stage 2	> 160	or	> 100
Hypertensive Crisis	> 180	or	> 110

Table 1.1: Blood Pressure Classifications. (The American Heart Association)

1.2.6. Risk Factors

Although the risk factors for cardiovascular disease are well known, adhering to the prevention guidelines is an issue in the U.S. Smoking, exercise, and a healthy diet are three major risk factors which can be easily self-controlled, however have been problematic. In 2007, 21-30% of children in grades nine through twelve reported some form of tobacco use and 17-22% of adults were cigarette smokers. 62% of adults reported no vigorous activity lasting more than ten minutes per session. The combination of physical inactivity and poor diet has led to increased obesity levels. Approximately 34% of U.S. adults are classified as obese (body mass index, BMI $\geq$ 30 kg/m^2). (Lloyd-Jones, et. al. 2008)

1.3. Windkessel Models

The German physiologist Otto Frank is credited with describing the hemodynamics of the arterial system by the Windkessel effect (Sagawa, et. al. 2004). "Windkessel" is a German word for "air bellow". It reflects the pumping of the heart when connected to the arterial system in systole and diastole.

The inflow of water to the pump via the canal in the model relates to the blood flow from the veins into the heart. The elastic distention of the aorta in systole corresponds to ventricular contraction. This is called arterial compliance. The blood viscosity in addition to small sized peripheral arteries contribute to total peripheral resistance. (Westerhof, et. al. 2008).

The chamber or Windkessel component of the circuit represents the interaction between the left ventricle, aortic valve, arterial vascular compartment, and peripheral

blood flow in the circulatory system (Westerhof, et. al. 2010). The left ventricle pumps blood out of the heart (cardiac output) and into the aorta. The blood pressure to blood volume relationship exhibited in the arterial compartment is measured as the compliance. The peripheral blood flow is governed by the arterial pressure and venous pressure and is measured as the resistance (reciprocal of conductance).

1.3.1. Resistance

The resistance, also called peripheral resistance (R_s), is the frictional resistance on blood flow by the blood vessels between the large arteries and right atrium. This includes the small arteries, arterioles, capillaries, venules, small veins, and veins (Sparks, et. al. 1987). The total peripheral resistance on blood flow can be determined using the change in pressure from the arterial side (P_a) to the venous side (P_v) compared to the cardiac output or blood flow (Q) (Li 2004).

$$R_s = \frac{P_a - P_v}{Q} \tag{1.3.1}$$

Poiseuille's law demonstrates that the influences on resistance include blood viscosity (π), vessel length (L), and vessel radius (r).

$$R = \frac{8\mu L}{\pi r^4} \tag{1.3.2}$$

Since resistance is inversely proportional to r^4, decreasing the vessel radius by only one half will result in a sixteen-fold increase in resistance. Thus, approximately 70% of the pressure change occurs in the small arteries and arterioles and 20% occurs in the capillaries (Sparks, et. al. 1987).

1.3.2. Compliance

Compliance (C) is a measure of a blood vessel's ability to resist recoil to its original dimensions upon the removal of a distending force. A highly compliant vessel can be easily stretched and is considered flexible, like a balloon. A noncompliant vessel cannot be easily stretched and is considered stiff, like a steel tube (Rhoades, et. al. 2013). In general, veins have a much higher compliance than arteries, mainly due to thinner walls. Compliance is expressed as the ratio of the change in blood volume (V) to the change in pressure (P) (Raff 2003).

$$C = \frac{\Delta V}{\Delta P} \tag{1.3.3}$$

Equation 1.3.3 indicates that arterial compliance is dependent on both volume and pressure. However, for many years arterial compliance has been considered a constant value since the change in compliance over physiological pressures is small. The linear, pressure-independent, constant arterial compliance value is obtained by,

$$C = \frac{-t_d}{\ln\left(P_d / P_{es}\right) R_s} \tag{1.3.4}$$

where t_d is the diastolic period, P_d is the diastolic pressure, and P_{es} is the end-systolic pressure (Matonick, et. al. 2001).

More recent studies show that more accurate results of modeling the arterial system can be accomplished with a nonlinear, pressure-dependent compliance element. This element, C(P) can be calculated as,

$$C(P) = ae^{-bP} \tag{1.3.5}$$

where *a* and *b* are constants. These constants can be derived from properties of the vascular system and parameter estimation. (Li, et. al. 1990).

1.3.3. Two-element Windkessel model

In order to gain further insight into the contributions of the various arterial properties, a quantitative model is necessary. Frank is credited with introducing the two-element Windkessel model (figure 1.1), which is an electrical analog representation of arterial circulation (Li 2004, Westerhof, et. al. 2008). The Windkessel model is considered a lumped model since it describes the complete arterial system by two discrete physiological parameters. In the circuit model, the blood pressure (P) and blood flow (Q) are analogous to voltage and current, respectively. The total peripheral resistance is represented by a resistor (R) and the artieral compliance is represented by a capacitor (C).

The two-element Windkessel model demonstrates the contribution of peripheral resistance and arterial compliance to the load on the heart (Stergiopulos, et. al. 1999). However, due to technological restrictions, Frank's model was based only upon aortic pressure.

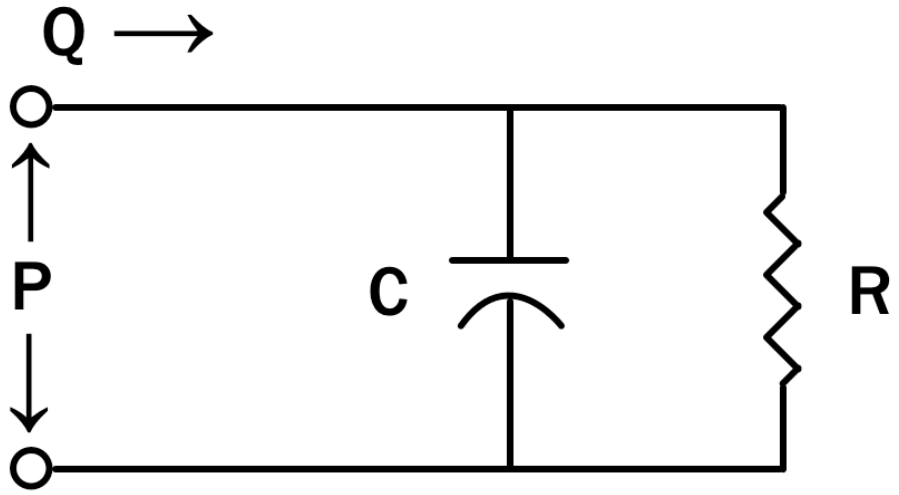

Figure 1.1: Two-element Windkessel model. The parameters are pressure, P, flow (current), Q, resistance (resistor), R, and compliance (capacitor), C.

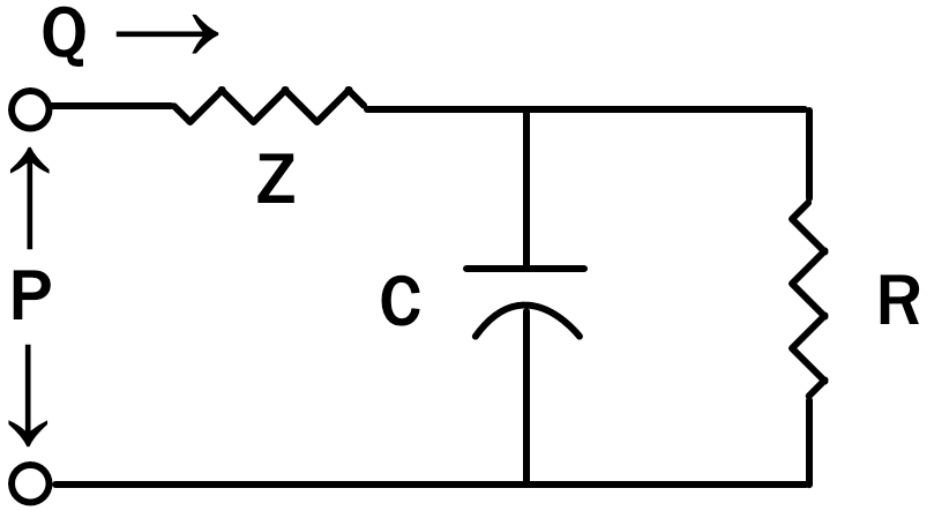

Figure 1.2: Three-element Windkessel model. The parameters are pressure, P, flow (current), Q, characteristic impedance (resistor), Z, resistance (resistor), R, and compliance (capacitor), C.

1.3.4. Three-element Windkessel model

When the technology to record blood flow measurements was developed, it was discovered that the input impedance of the two-element model varied significantly from the actual impedance at high frequencies. The model did not take into account the resistance to blood flow experienced within the heart due to the aortic and pulmonary valves or reflected pressure waves. A modified three-element Windkessel model was proposed by Nicolaas Westerhof. This model accounted for peripheral resistance, arterial compliance, and characteristic impedance of the proximal aorta (Jaffrin 1995, Westerhof, et. al. 1971).

A second resistor (Z) was added to the circuit to represent the characteristic impedance (Z_0). Figure 1.2 shows the three-element Windkessel model. While the addition of a resistor for characteristic impedance improves the accuracy of the Windkessel model at high frequencies, it also creates small errors at low frequency ranges of input impedance (Westerhof, et. al. 2008).

1.3.5. Four-element Windkessel model

The errors at low frequency ranges exhibited by the three-element Windkessel can be attributed to the neglect of total arterial inertance (effect of inertia) on the system (Burattini, et. al. 1982). This model did not account for compliance and inertance beyond the proximal aorta. The four-element Windkessel model adds an inductor (L) to the circuit to represent the total arterial inertance (figure 1.3, Westerhoff, et. al. 2004).

While the four-element Windkessel model provides the most accurate representation of the arterial system, recent studies have shown that the inertance is

difficult to estimate (Segers, et. al. 2005, Westerhof, et. al. 2008). Despite the errors at low frequencies, the three-element Windkessel is a good model of the arterial system. The three-element Windkessel remains the preferred model since the difficulty in estimating inertance provides only a minimal improvement on accuracy.

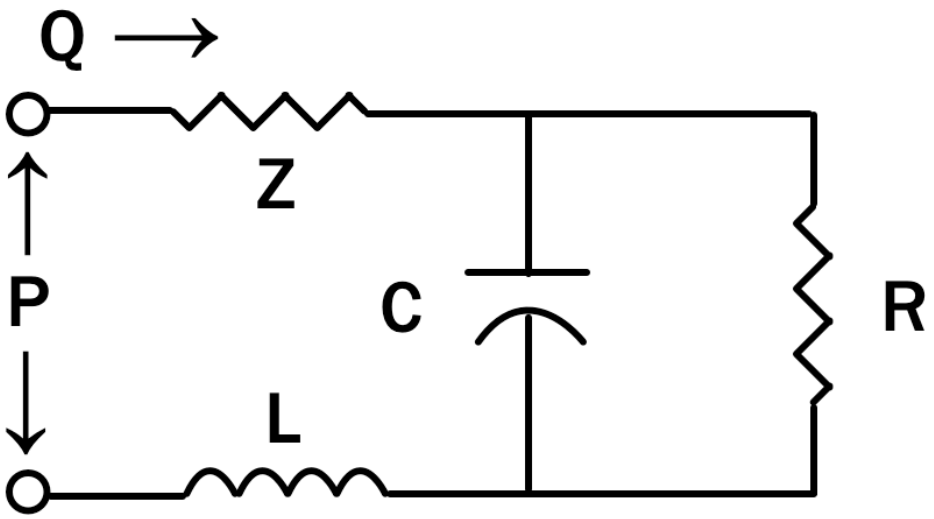

Figure 1.3: Four-element Windkessel model. The parameters are pressure, P, flow (current), Q, characteristic impedance (resistor), Z, resistance (resistor), R, compliance (capacitor), C, and inertance (inductor), L.

1.4. Augmentation Index

The aortic pressure waveform is the sum of the forward pressure wave and reflected (backward) pressure wave (figure 1.4b). The forward pressure wave (P_f) is generated by ventricular ejection of blood from the heart. The reflected pressure wave (P_r) is generated by an impedance mismatch in the peripheral arterial tree (Shimizu, et. al. 2008). After left ventricular ejection the forward wave propagates from the heart to the peripheral arterial tree. At arterial bifurcations and arteriolar beds the propagating wave is reflecting, generating a reflected wave that propagates back to the heart. The point where the forward and reflected waves merge affect the level of the central blood pressure (Segers, et. al. 2001).

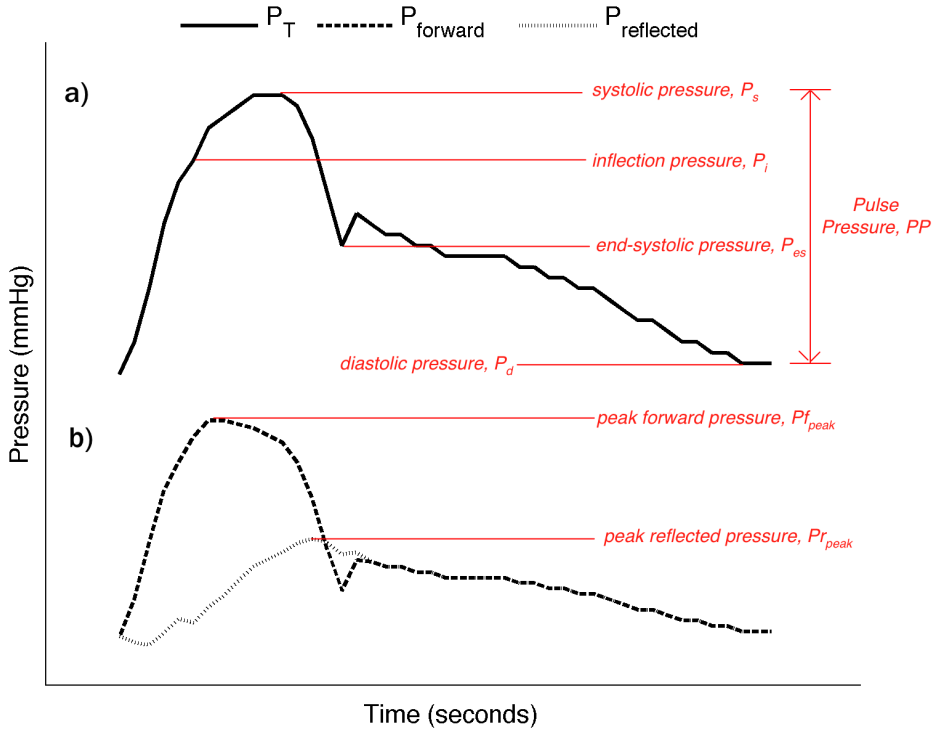

Figure 1.4: Pressure pulse wave parameters. (a) Pressure pulse wave. (b) Forward and reflected pressure pulse waves.

Augmentation index (AIx) is an indicator of the accentuation of systolic pressure due to the reflected wave. (Nürnberger, et. al. 2002). Physiologically, arterial stiffness is represented by augmentation index. The current method of determining augmentation index is the ratio of augmentation pressure (AP) to pulse pressure (PP) (Murgo, et. al. 1980).

$$AIx = \frac{\text{Augmentation Pressure}}{\text{Pulse Pressure}} \tag{1.4.1}$$

Augmentation pressure is a measure of the effect that the reflected wave has on the systolic arterial pressure. The contribution is determined be measuring the propagation of the reflected wave moving from the periphery to the center. Augmentation pressure is calculated by determining the difference between the systolic pressure (P_s) and inflection pressure (P_i) (figure 1.4a).

$$AP = P_s - P_i \tag{1.4.2}$$

Pulse pressure is the pressure caused by the blood against the walls of the arteries. It is calculated by determining the difference between the systolic and diastolic pressure (P_d).

$$PP = P_s - P_d \tag{1.4.3}$$

Low arterial compliance will cause the reflected wave to reach the heart in the systolic phase rather than the diastolic phase. The early arrival causes an uneven rise in systolic blood pressure and pulse pressure resulting in an increase in afterload and a decrease in preload. (Fantin, et. al. 2007).

Studies have shown that augmentation index is useful in determining cardiovascular risk (Nürnberger, et. al. 2002). Increased arterial stiffness leads to a faster forward pulse wave and a subsequent faster reflected wave. Various other factors have

also been shown to influence augmentation index. Body height represents the distance the forward wave must travel to reach the major reflecting sites. An increased heart rate causes a shorter ejection duration leading to a late reflected wave. Recent studies have indicated that augmentation index increases with age due to the progression of arterial stiffness (McEniery, et. al. 2005). In younger subjects there is a steep increase, while older subjects (fifty to sixty years old) exhibit a gradual increase that eventually plateaus. Some studies have shown high augmentation index to be linked with target organ damage such as hypertrophy of the left ventricle and aortic atherosclerosis (Saba, et. al. 1993, Qureshi, et. al. 2007), while other studies have found no significant correlation, indicating a need for further examination (Shimizu, et. al. 2008).

Chapter 2: Aims and Significance

Cardiovascular diseases are the number one cause of death in the world. According to the World Health Organization, cardiovascular diseases were responsible for 17.3 million deaths in 2008 and will increase to an estimated 23.6 million deaths annually by 2030. The most important risk factor for the majority of these diseases is hypertension. Stroke, a type of cardiovascular disease, is the number one cause of serious and long-term disability in the United States. Myocardial ischemia is the most common cause of stroke.

Prevention of cardiovascular diseases is dependent on limiting the risk factors, early detection, and early treatment. Early detection and treatment of the important risk factors, hypertension and myocardial ischemia, will delay or prevent the development of heart failure and stroke.

The current method for monitoring hypertension relies solely on blood pressure. A patient is classified as normal, prehypertensive, stage 1 hypertensive, stage 2 hypertensive, or in hypertensive crisis based upon their systolic and diastolic blood pressure measurements. Their risk for cardiovascular diseases and treatment intensity is dependent on their classification. While blood pressure provides a broad overview of the cardiovascular system, clinicians should utilize more sophisticated cardiac markers for diagnosis and determining potential risk. This thesis investigates the effect of hypertension and myocardial ischemia on other possible cardiac parameters.

First, the effect of hypertension and myocardial ischemia on blood pressure and blood flow is confirmed. The change in systolic and diastolic blood pressures is analyzed. Additionally, the pressure pulse wave is separated into a forward pressure wave and

reflected pressure wave to further understand the effect of hypertension and myocardial ischemia on blood pressure. Arterial compliance is an alternative parameter that could provide insight into a patient's risk for a cardiovascular event. Currently the three-element Windkessel model is the preferred model for the arterial system. The accuracy of the model using a linear, pressure-independent compliance parameter is compared to the use of a nonlinear, pressure-dependent compliance parameter. The continuous changing arterial compliance in terms of arterial blood pressure is investigated.

Lastly, in order to investigate potential flaws or deficiencies in the current augmentation index calculation, it is compared to four new calculation methods. The ability of each method to distinguish between a control group, hypertension group, and vasodilation group is examined. The outcome should confirm the effectiveness of using the current calculation for determining cardiovascular risk or indicate a better method. The change in the five augmentation index parameters in myocardial ischemia is also investigated to determine if augmentation index can be extended to provide potential risk data for other specific cardiovascular diseases.

Chapter 3: Methods

3.1. Data Acquisition

The experimental data was obtained from mongrel dogs in experiments conducted by Dr. John K-J Li (Li, et. al. 1990, Matonick, et. al. 2001). The experiments were conducted on anesthetized dogs (30 mg/kg IV of Nembutal) that weighed between 20 to 24 kg. Respiration was maintained and monitored throughout the procedure by tracheal intubation and an external ventilator. The aorta was approached through a left thoracotomy and cuffed with an electromagnetic flow probe. Left ventricular pressure and aortic pressure were simultaneously measured with a Millar type catheter-tip transducer. The aortic pressure, aortic flow, left ventricular pressure, and standard lead II electro cardiogram were continuously recorded and sampled at 10 ms intervals by a computer.

This protocol was used to obtain data for the four conditions: control, hypertension, vasodilation, and myocardial ischemia. Spontaneous hypertension was induced through intravenous injections of methoxamine (MTX) in bolus dosages of 5 mg/mL. Spontaneous vasodilation was induced through intravenous injections of sodium nitroprusside (NTP) in bolus dosages of 10 mg/mL. Myocardial ischemia was induced by imposing a mechanical occlusion of the left anterior descending coronary artery just below the first major branching for one hour.

Methoxamine is a potent alpha-1 adrenergic receptor agonist that is commonly used to treat hypotension or shock (Frishman, et. al. 2005). Activation of the alpha-1 adrenergic receptors causes vasoconstriction of arties and veins and contraction of

smooth muscle. These reactions lead to an increase in systolic and diastolic blood pressure, which are good simulations of hypertension (Smith, et. al. 2011). Methoxamine has an onset of action after intravenous administration of 0.5 to 2 minutes and its duration of action is approximately 10 to 15 minutes. After injection, there will be an increase in systolic and diastolic blood pressures for 60 to 90 minutes (Dart 2004).

Sodium nitroprusside is a potent vasodilator that is commonly used to treat hypertensive crisis or acute congestive heart failure. The drug interacts with the sulphydryl groups in the smooth muscle membrane, preventing the calcium ion influx that is necessary for contraction. The inhibition of contraction causes the vasodilation of blood vessels (Smith, et. al. 2011). Sodium nitroprusside has an almost immediate onset of action after intravenous administration and its duration of action is approximately 1 to 10 minutes (Frishman, et. al. 2005).

3.2. Pressure Pulse Waveform

The pressure waveform data is plotted against time and the parameters shown in figure 1.4a are calculated. The systolic pressure (P_s) is the largest pressure value and the diastolic pressure (P_d) is the smallest pressure value. The end-systolic pressure (P_{es}) is the pressure at the end of systole. The pulse pressure (PP) is the difference between systolic pressure and diastolic pressure (equation 1.4.3). The inflection pressure (P_i) is the pressure at peak blood flow (Q) and represents the first upstroke of the reflected pressure wave (O'Rourke, et. al. 2010).

The characteristic impedance (Z_0) is the ratio of the change in pressure over the change in flow between each discrete sample for the first sixty milliseconds of the

pressure waveform. The impedance is the mean of the six resulting values (Z_0, Z_1, …, Z_6). (Westerhof, et. al. 2008)

$$Z_0 = \frac{\Delta P}{\Delta Q} = \frac{1}{6}\left(\sum_{n=1}^{6} \frac{P_{n+1} - P_n}{Q_{n+1} - Q_n}\right) \tag{3.2.1}$$

The pressure pulse waveform is the sum of the forward pressure wave (P_f) and reflected pressure wave (P_r), shown in figure 1.4b (Li, et. al. 2010).

$$P = P_f + P_r \tag{3.2.2}$$

The forward pressure wave is calculated by,

$$P_f = \frac{1}{2}\left(P + QZ_0\right) \tag{3.2.3}$$

and the reflected pressure wave is calculated by,

$$P_r = \frac{1}{2}\left(P - QZ_0\right) \tag{3.2.4}$$

The total pressure, forward pressure, and reflected pressure waveforms were plotted against time. The blood flow waveforms were plotted against time as well. The software tool MATLAB 7.9 (R2009b) was used for all calculations and to generate the plots.

3.3. Three-element Windkessel Model

The three-element Windkessel model was chosen to represent the arterial system (figure 1.2). Estimating the inertance parameter for the four-element Windkessel proves to be difficult and only provides a minimal improvement in accuracy. At physiologically based parameters, the three-element Windkessel is the preferred model for the arterial system (Westerhof, et. al. 2008).

Recall that the total peripheral resistance (R_s) on blood flow is the ratio of the change in pressure between the arterial (P_a) and venous side (P_v) over the blood flow (Q) (equation 1.3.1). At steady flow the assumption can be made that the venous pressure is small and can be neglected. Thus, the calculation for peripheral resistance is the ratio of the mean arterial pressure ($\overline{P}$) to mean arterial flow ($\overline{Q}$).

$$R_s = \frac{\overline{P}}{\overline{Q}} \tag{3.3.1}$$

The circuit seen in figure 1.2 for the three-element Windkessel model shows that the total blood flow is the sum of the flow through the compliance branch (Q_C) and the flow through the resistance branch (Q_R).

$$Q(t) = Q_C(t) + Q_R(t) \tag{3.3.2}$$

The blood flow through the compliance branch is given by,

$$Q_C(t) = C \cdot \frac{dP(t)}{dt} \tag{3.3.3}$$

and the blood flow through the resistance branch is given by,

$$Q_R(t) = \frac{P(t)}{R_s} \tag{3.3.4}$$

Equating and rearranging equations 3.3.3 and 3.3.4 yields,

$$\frac{dP(t)}{dt} = \frac{1}{C}\left(Q(t) - \frac{P(t)}{R_s}\right) \tag{3.3.5}$$

Using difference representations and discrete analysis, equation 3.3.5 can be reduced to

$$P(t_{n+1}) = P(t_n) + \frac{\Delta t}{C}\left(Q(t_n) - \frac{P(t_n)}{R_s}\right) \tag{3.3.6}$$

where Δt is the sampling interval, which in this case is ten milliseconds. Using the solution, $P(t_n)$ obtained from equation 3.3.6 with the measured blood flow, the predicted pressure waveform can be calculated using,

$$P_a(t_n) = P(t_n) + Q(t_n)Z_0 \tag{3.3.7}$$

Two methods were utilized to calculate compliance for the three-element Windkessel model. The first method treated compliance as a linear, pressure-independent parameter (equation 1.3.4). The diastolic period (t_d) is calculated by determining the time difference between the diastolic pressure and end-systolic pressure.

The second method treated compliance as a non-linear, pressure-dependent parameter (equation 1.3.5). The values of the constants, *a* and *b,* were determined by parameter estimation. Previous experiments on canine subjects have shown that in a normal arterial system, the zero pressure compliance is in the range of 1 to 1.4 mL/mmHg. Thus the physiological range for the value of *a* in the control system is 1 to 1.4. Additionally the range of *a* in a hypertensive system is 0.65 to 1 and in a vasodilated system is 2 to 3 (Matonick, et. al. 2001).

In order to determine the exact value of each constant, a range of values were tested and the best-fit Windkessel parameters were chosen. The test values for *a* were chosen within the ranges outlined above. For the ischemic condition a broad range from 0.65 to 3 was chosen. The first estimate for *b* was obtained by solving equation 1.3.5 using the median value of *a* and substituting the linear compliance value from equation 1.3.4 for C(P) and the mean arterial pressure for P. The additional test values for *b* were determined by taking a range values from ±25% of the initial estimation. In order to determine which set of constants provided the best-fit Windkessel model, an error value

was calculated between the predicted pressure and measured pressure waveforms. The pair of constants yielding the lowest error value were chosen as the best-fit parameters. The error value was calculated using a root mean square error technique:

$$E = \sqrt{\frac{1}{n}\sum_{i=1}^{n}\left(P_{pred} - P_{meas}\right)^2} \tag{3.3.8}$$

Two predicted pressure waveforms were generated for each dataset using the pressure-independent and pressure-dependent compliance parameters (Matonick, et. al. 2001, Li, et. al. 1990).

Multiple plots were generated to compare the data obtained from the implementation of the Windkessel model. The nonlinear, pressure-dependent compliance and measured pressure wave were plotted against time. The nonlinear, pressure-dependent compliance was plotted against pressure to visualize the pressure-compliance loop. The measured pressure waveform and the two predicted pressure waveforms (from pressure-independent and pressure-dependent compliance) were plotted against time. The software tool MATLAB 7.9 (R2009b) was used for all calculations and to generate the plots.

3.4. Augmentation Indices

Recall, the current method of determining augmentation index from equation 1.4.1. For each dataset, augmentation index was calculated using five different methods. The parameters used in the five equations are shown in figure 3.1. The first method, denoted AIx_1, uses the currently accepted equation.

$$AIx_1 = \frac{P_s - P_i}{P_s - P_d} \tag{3.4.1}$$

AIx_1 is calculated by comparing the ratio of the difference between the systolic pressure (P_s) and inflection pressure (P_i) to the difference between the systolic pressure and diastolic pressure (P_d). The second method, denoted AIx_2, is the ratio of the peak reflected pressure ($P_{r,\,peak}$) to the peak forward pressure ($P_{f,\,peak}$).

$$AIx_2 = \frac{P_{r,\,peak}}{P_{f,\,peak}} \tag{3.4.2}$$

The third method, denoted AIx_3, is the ratio of the reflected pressure at peak forward pressure ($P_{r,f}$) to the peak forward pressure.

$$AIx_3 = \frac{P_{r,f}}{P_{f,\,peak}} \tag{3.4.3}$$

The fourth method, denoted AIx_4, is the ratio of the reflected pressure at systolic pressure ($P_{r,\,s}$) to the forward pressure at systolic pressure ($P_{f,\,s}$).

$$AIx_4 = \frac{P_{r,\,s}}{P_{f,\,s}} \tag{3.4.4}$$

The fifth method, denoted AIx_5, is the ratio of the difference between systolic pressure and inflection pressure to the inflection pressure.

$$AIx_5 = \frac{P_s - P_i}{P_i} \tag{3.4.5}$$

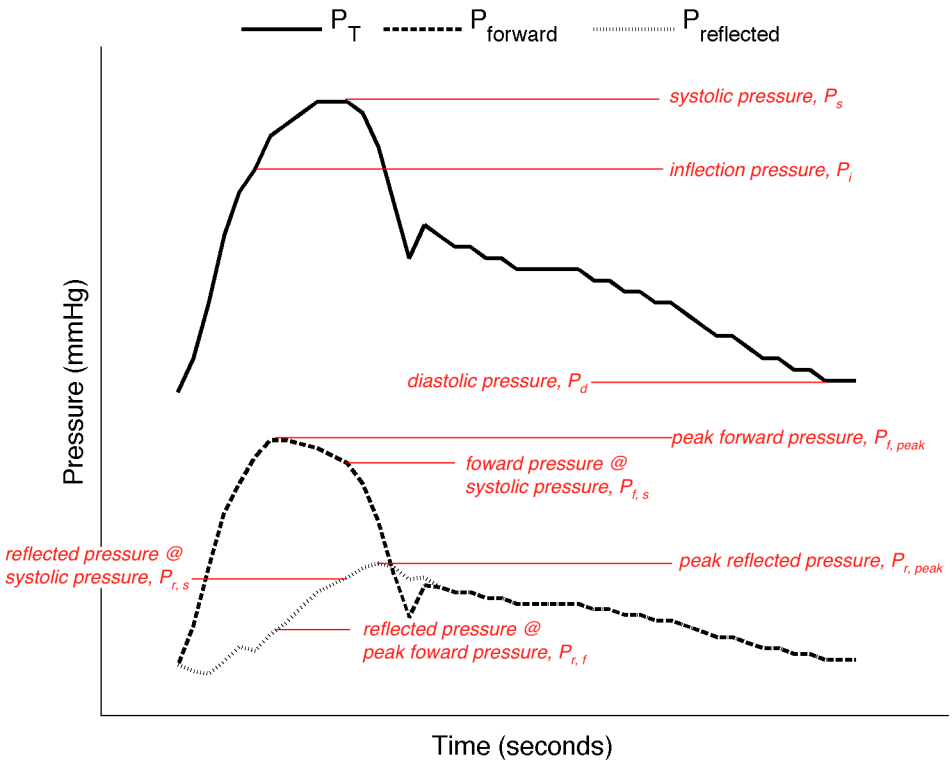

Figure 3.1: Augmentation index parameters.

Chapter 4: Results

Each dataset corresponds to measurements recorded from a single dog. Datasets 1 and 2 contain control, hypertension (MTX), and vasodilation (NTP) data. Dataset 3 only has data for control and vasodilation, while dataset 4 only has data for hypertension and vasodilation. This data is used to compare the effect vasoconstriction and vasodilation have on various arterial parameters. Datasets 5 to 7 contain control and ischemia data. This data is used to compare the effect ischemic conditions have on the same arterial parameters.

The tables presented in this chapter represent the numerical results of the calculations described in chapter three (methods) for all seven datasets. In instances where the comparison plots from different datasets produce similar results, only a select sample of plots are shown. The selected plots exhibit similar patterns to the omitted plots and provide a sufficient representation of the collective results.

4.1. Pressure and Flow Waveforms

The measured pressure pulse wave was plotted with the forward and reflected pressure waves against time. Figures 4.1-4.3 show the waveforms for control, hypertension, and vasodilation. The systolic and diastolic pressures increase in hypertension and decrease in vasodilation compared to the control pressure waveform. Additionally the ratio of peak reflected pressure to peak forward pressure increases in hypertension and decreases in vasodilation compared to the control waveforms. Figures 4.4 and 4.5 show the waveforms for control and ischemia. The systolic and diastolic

pressures decrease in ischemia compared to control. The numerical values for all the datasets are presented in tables 4.1 and 4.2.

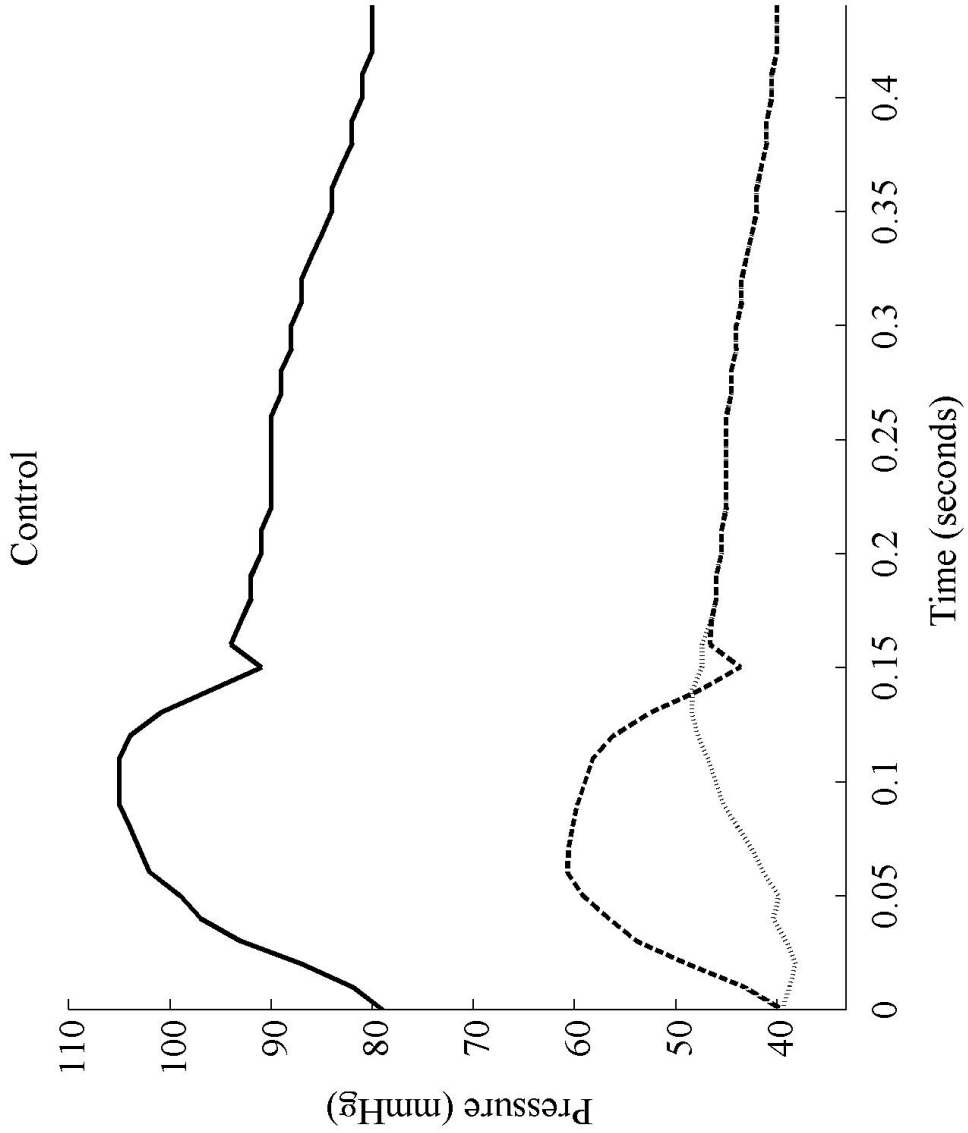

Figure 4.1: Pressure waveforms for control condition (dataset 1). A comparison of the total pressure, forward pressure, and reflected pressure waveforms. Solid line: total pressure; Dashed line (---): forward pressure; Dotted/grey line (⋯): reflected pressure.

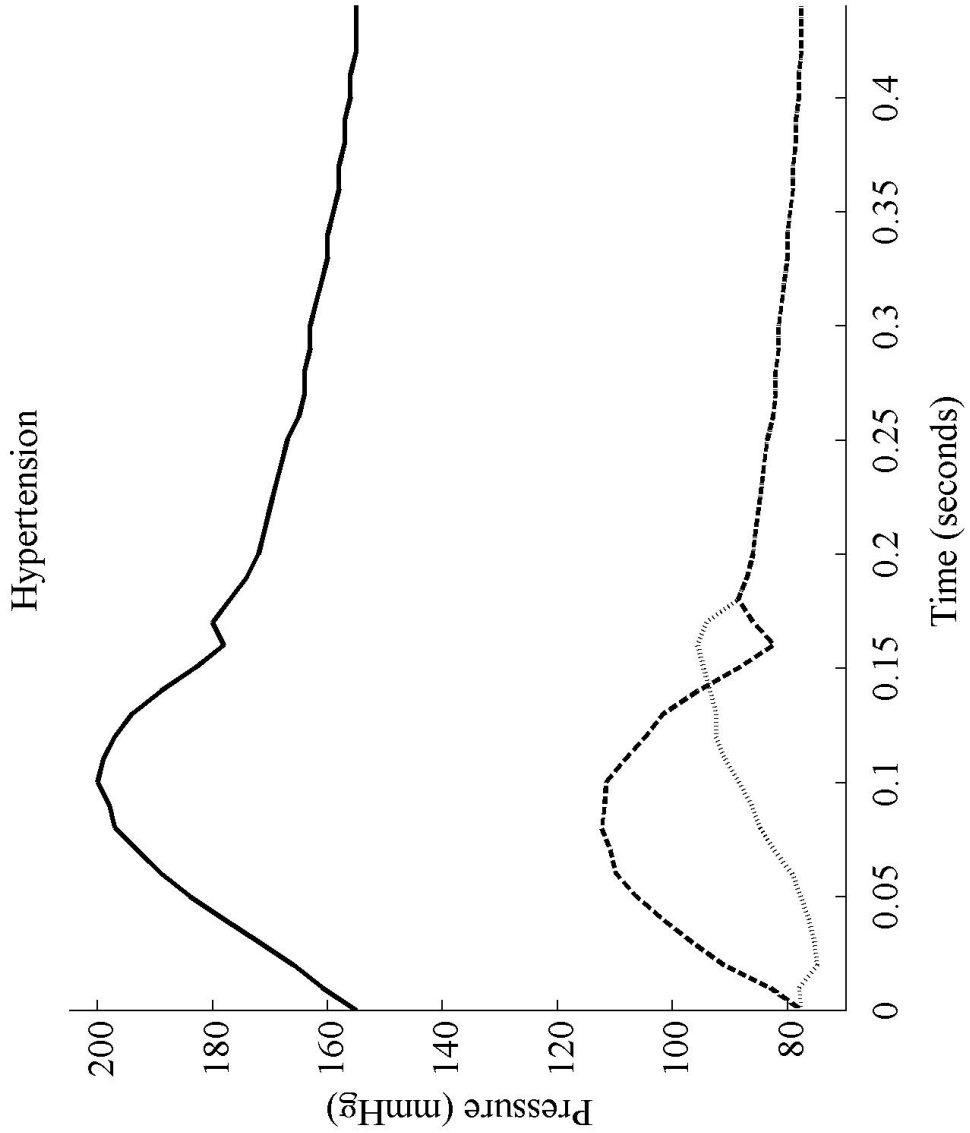

Figure 4.2: Pressure waveforms for hypertension condition (dataset 1). A comparison of the total pressure, forward pressure, and reflected pressure waveforms. Solid line: total pressure; Dashed line (---): forward pressure; Dotted/grey line (⋯): reflected pressure.

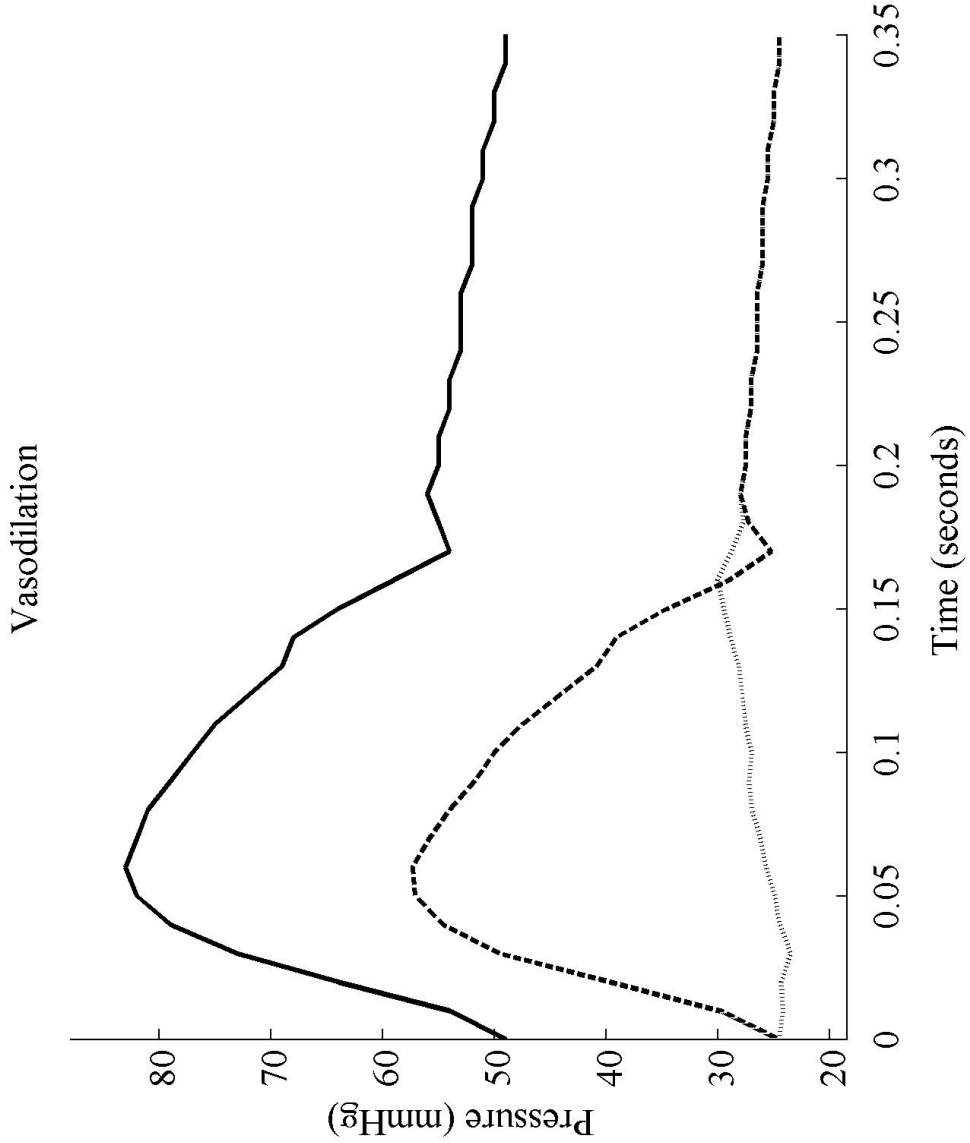

Figure 4.3: Pressure waveforms for vasodilation condition (dataset 1). A comparison of the total pressure, forward pressure, and reflected pressure waveforms. Solid line: total pressure; Dashed line (---): forward pressure; Dotted/grey line (⋯): reflected pressure.

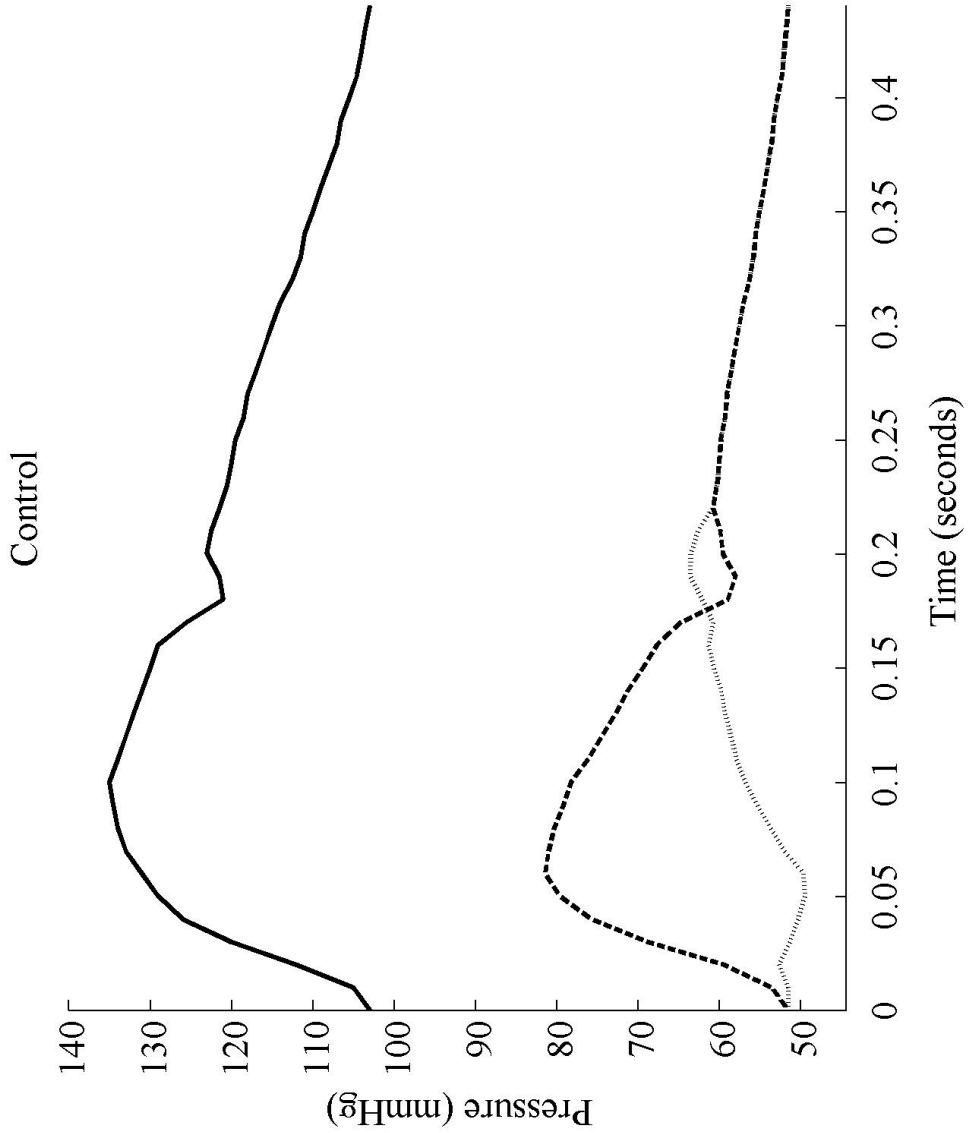

Figure 4.4: Pressure waveforms for control condition (dataset 5). A comparison of the total pressure, forward pressure, and reflected pressure waveforms. Solid line: total pressure; Dashed line (---): forward pressure; Dotted/grey line (⋯): reflected pressure.

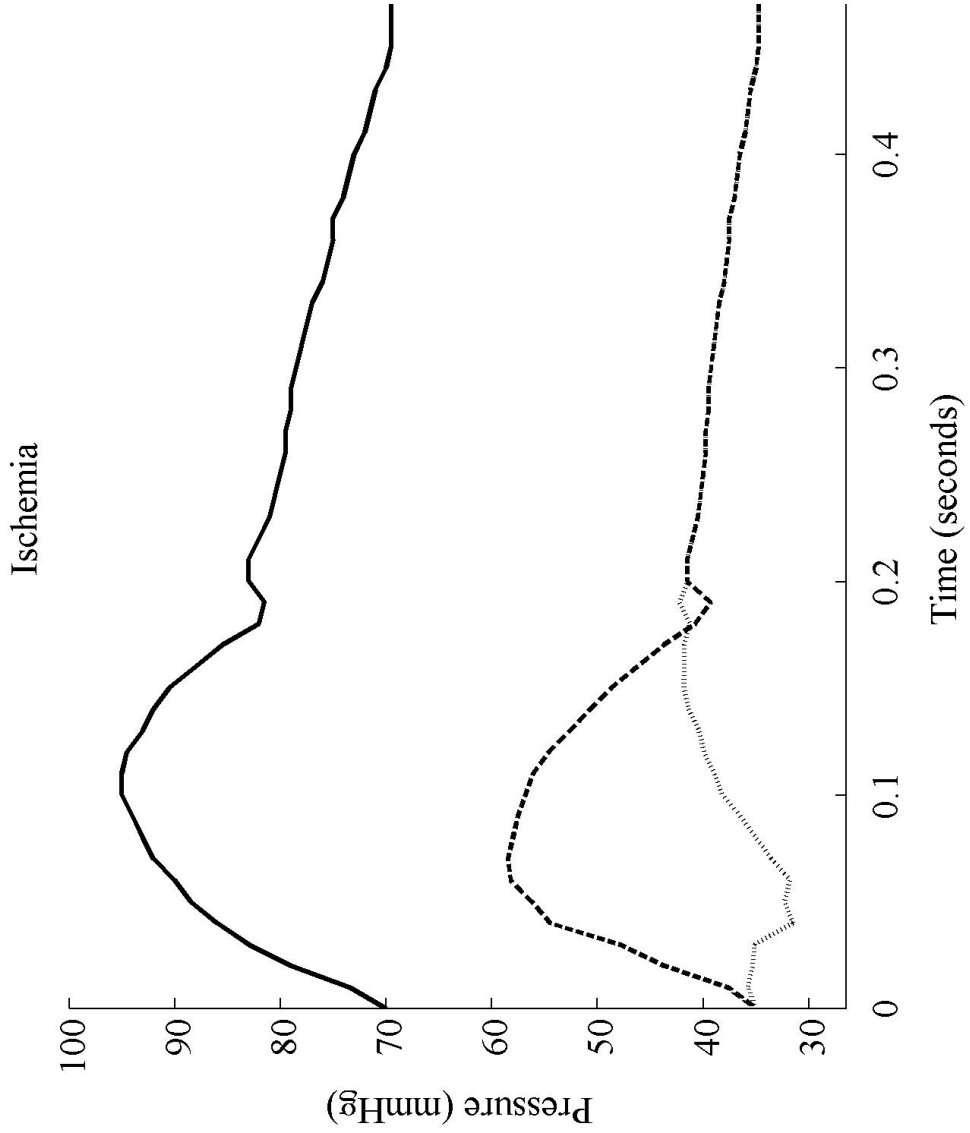

Figure 4.5: Pressure waveforms for ischemia condition (dataset 5). A comparison of the total pressure, forward pressure, and reflected pressure waveforms. Solid line: total pressure; Dashed line (---): forward pressure; Dotted/grey line (⋯): reflected pressure.

Dataset	Systolic Pressure (P_s)			Diastolic Pressure (P_d)			Blood Flow (Q)		
	Control	MTX	NTP	Control	MTX	NTP	Control	MTX	NTP
1	105	200	83	79	155	49	102	90	126
2	132	156	96	105	123	67	100	102	152
3	114	-----	74	90	-----	56	92	-----	105
4	-----	180	104	-----	144	78	-----	104	140
Mean	117.0	178.7	89.3	91.3	140.7	62.5	98.0	98.7	130.8
St. Dev.	13.75	22.03	13.35	13.05	16.25	12.71	5.29	7.57	20.19

Dataset	Peak Forward Pressure ($P_{f,\,peak}$)			Peak Reflected Pressure ($P_{r,\,peak}$)		
	Control	MTX	NTP	Control	MTX	NTP
1	61	112	57	48	96	30
2	75	84	63	60	76	35
3	67	-----	46	54	-----	31
4	-----	98	64	-----	88	43
Mean	67.7	98.0	57.5	54.0	86.7	34.8
St. Dev.	6.93	14.18	8.35	5.83	9.97	6.07

Table 4.1: Systolic pressure, diastolic pressure, blood flow, peak forwards pressure, and peak reflected pressure (datasets 1-4). "*MTX"*: hypertension condition; "*NTP"*: vasodilation condition. Pressure units: mmHg; blood flow units: mL/s.

Dataset	Systolic Pressure (P_s)		Diastolic Pressure (P_d)		Blood Flow (Q)		Peak Forward Pressure ($P_{f,\,peak}$)		Peak Reflected Pressure ($P_{r,\,peak}$)	
	Control	I	Control	I	Control	I	Control	I	Control	I
5	135	95	103	70	160	108	81	58	64	42
6	92	87	70	68	108	74	57	53	41	41
7	99	94	82	78	148	126	54	53	47	43
Mean	108.7	92.0	85.0	72.0	138.7	102.7	64.0	54.7	50.7	42.0
St. Dev.	23.07	4.25	16.70	5.01	27.23	26.41	14.77	3.26	11.82	1.10

Table 4.2: Systolic pressure, diastolic pressure, blood flow, peak forwards pressure, and peak reflected pressure (datasets 5-7). *"I"*: ischemia condition. Pressure units: mmHg; blood flow units: mL/s.

The measured blood flow waveforms were plotted against time. Figure 4.6 shows the waveforms for control, hypertension, and vasodilation plotted together. The peak blood flow decreases in hypertension and increases in vasodilation compared to the control blood flow. Figure 4.7 shows the waveforms for control and ischemia. The peak blood flow decreases in ischemia.

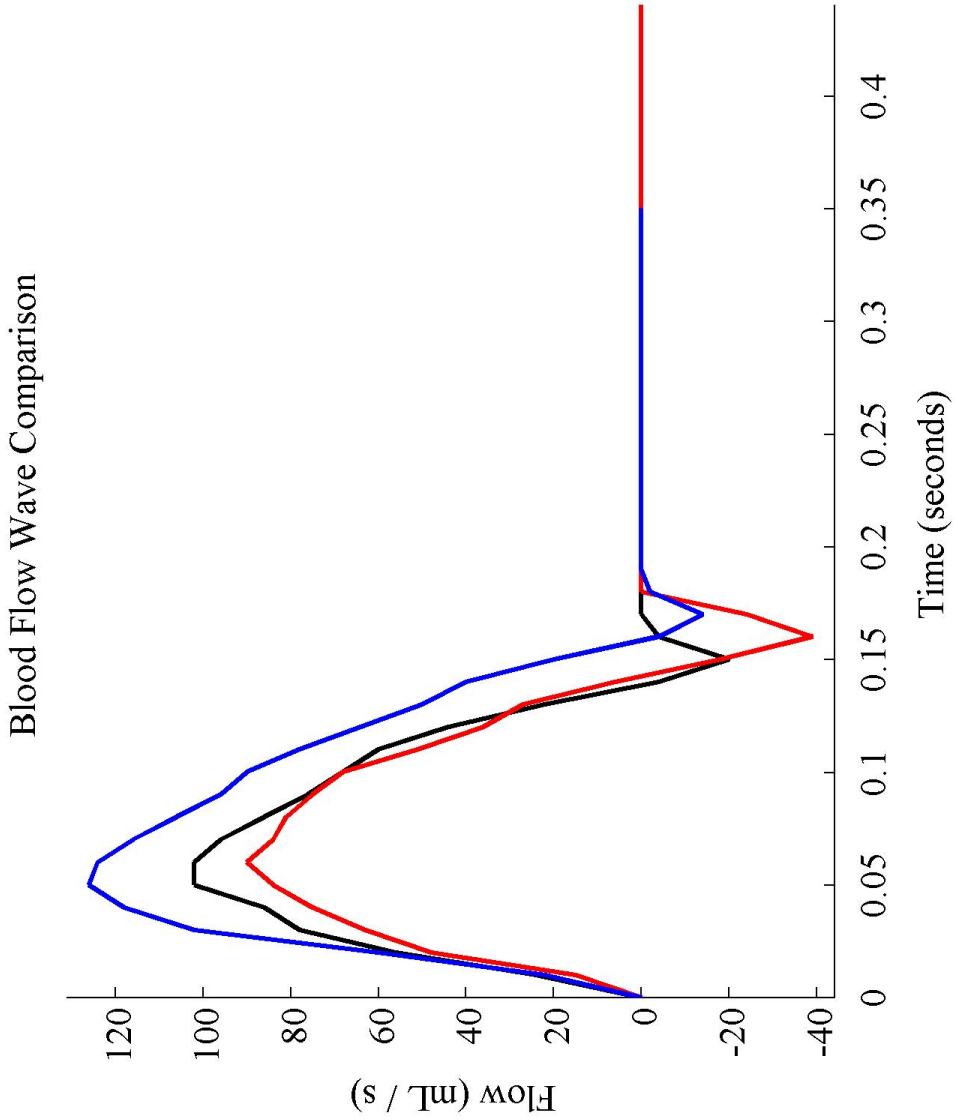

Figure 4.6: Blood flow waveforms for control, hypertension, and vasodilation conditions (dataset 1). Black line: control condition; red line: hypertension condition; blue line: vasodilation condition.

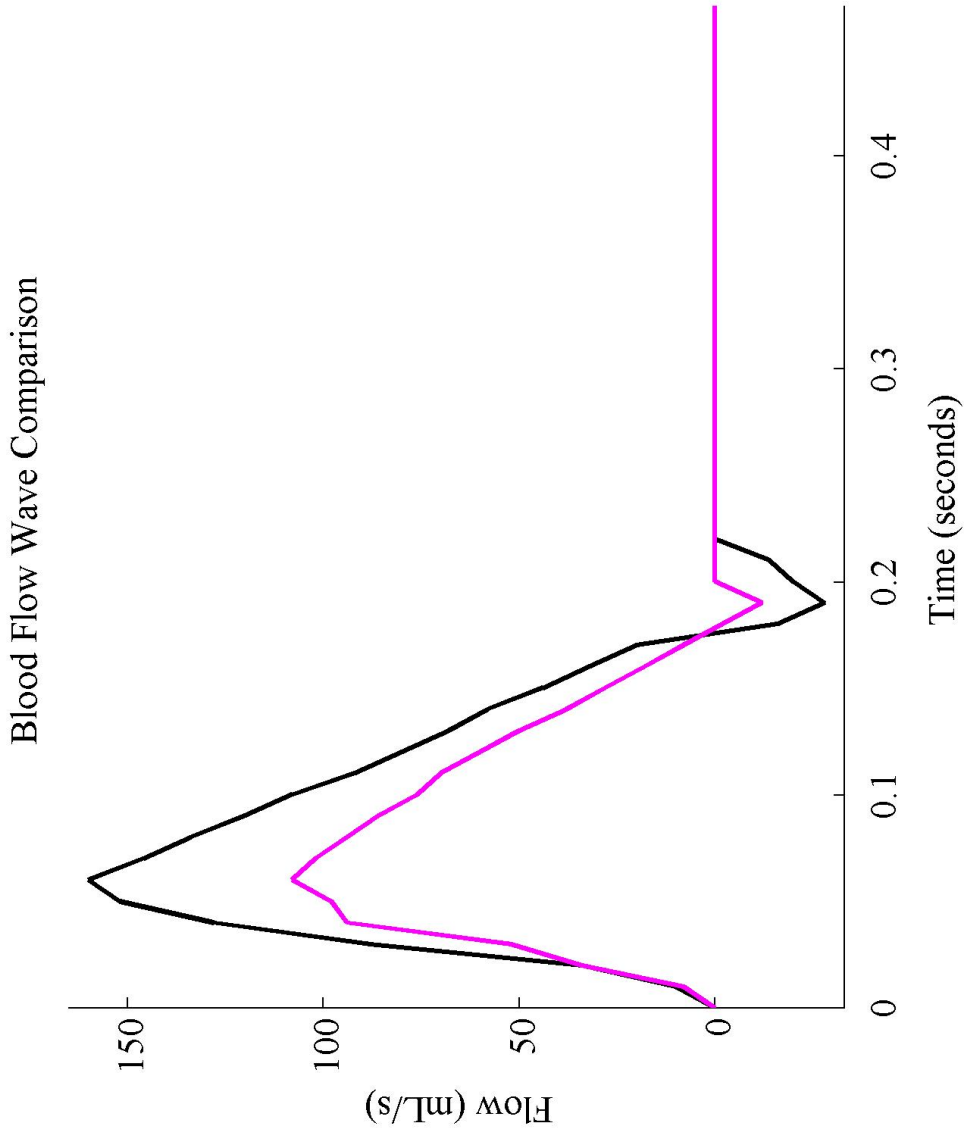

Figure 4.7: Blood flow waveforms for control and ischemia conditions (dataset 5).

Black line: control condition; pink line: ischemia condition.

4.2. Compliance-Pressure Relationship

In order to investigate the relationship between compliance and pressure, three types of plots were generated. First, the measured pressure was compared with the predicted pressure calculated from the linear (pressure-independent compliance) and non-linear (pressure-dependent compliance) three-element Windkessel models. The closer the predicted pressure wave is to the measured pressure wave, the more accurate the model. Figures 4.8-4.10 show the plots for control, hypertension, and vasodilation, respectively. Figures 4.11 and 4.12 show the plots for control and ischemia, respectively. In all instances the non-linear compliance model appears to provide a more accurate pressure prediction than the linear compliance model. The root mean square error between the predicted pressure and the two compliance models are presented in tables 4.3 and 4.4. The compliance method with the lower error value can be considered the more accurate Windkessel model.

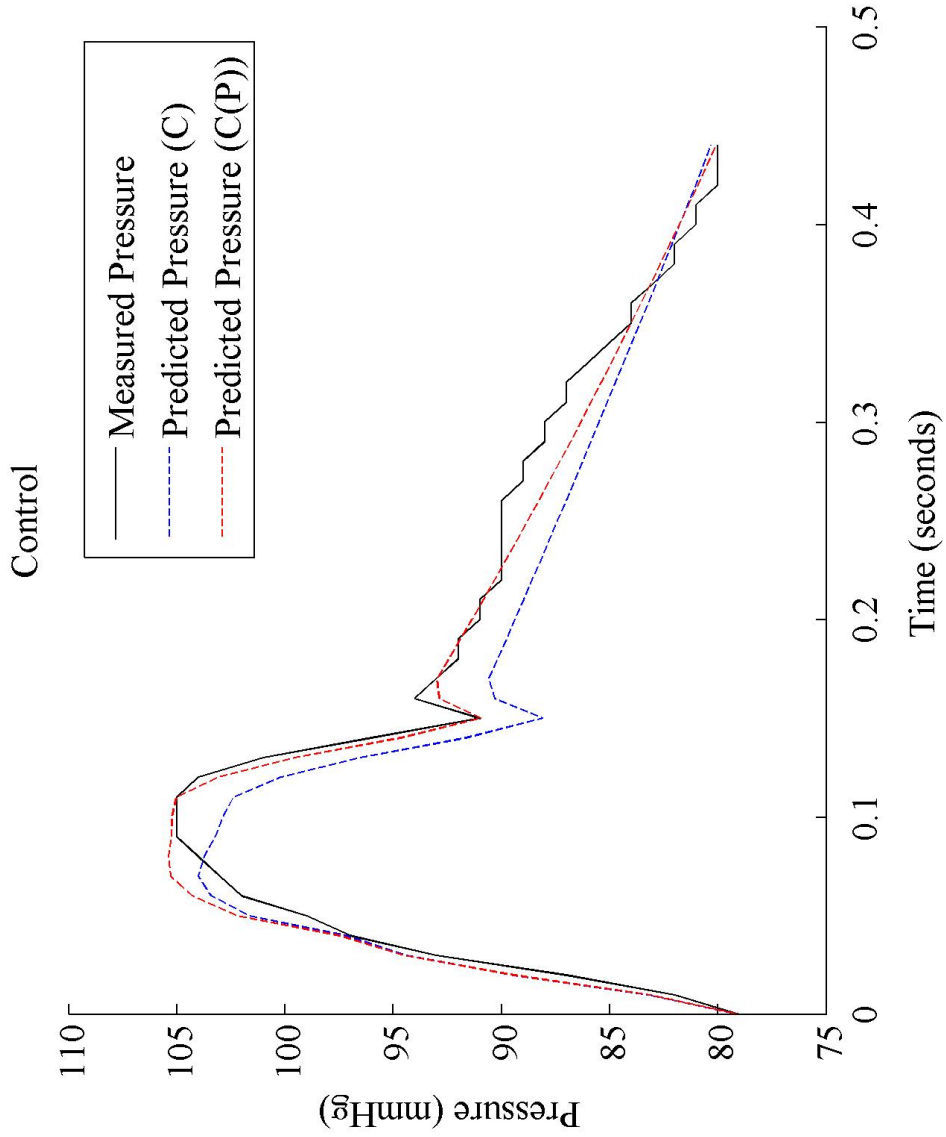

Figure 4.8: Predicted vs. measured pressure for control condition (dataset 1). Black solid line: measured pressure; blue dashed line: predicted pressure from linear compliance model; red dashed line: predicted pressure from non-linear compliance model.

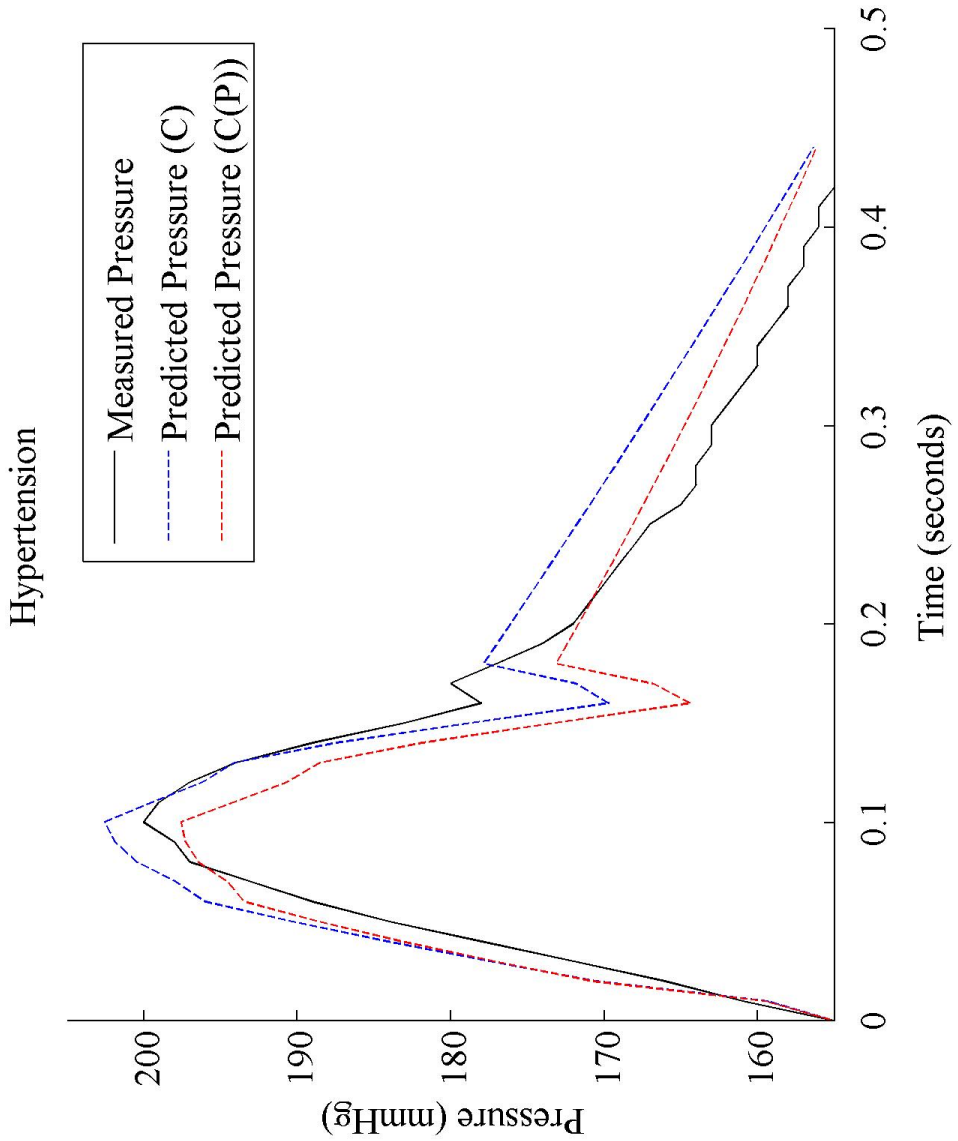

Figure 4.9: Predicted vs. measured pressure for hypertension condition (dataset 1). Black solid line: measured pressure; blue dashed line: predicted pressure from linear compliance model; red dashed line: predicted pressure from non-linear compliance model.

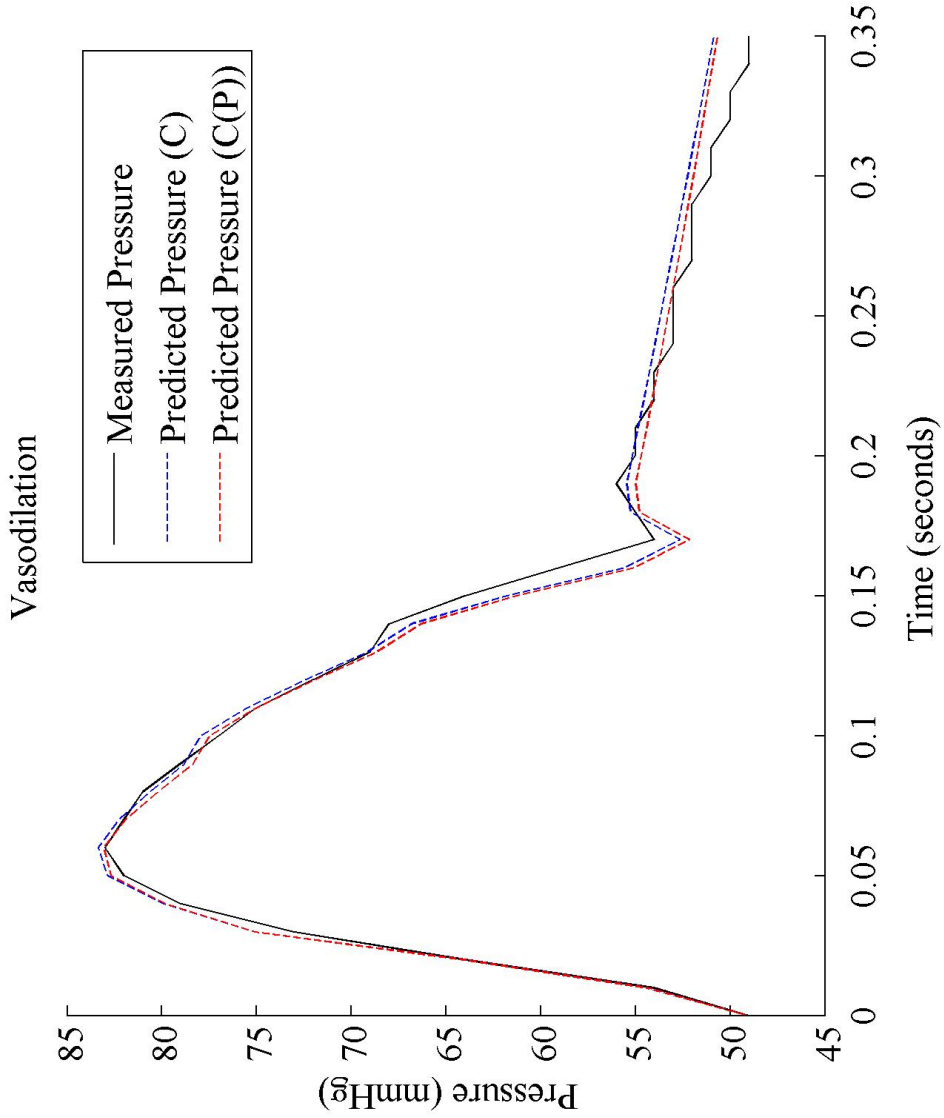

Figure 4.10: Predicted vs. measured pressure for vasodilation condition (dataset 1). Black solid line: measured pressure; blue dashed line: predicted pressure from linear compliance model; red dashed line: predicted pressure from non-linear compliance model.

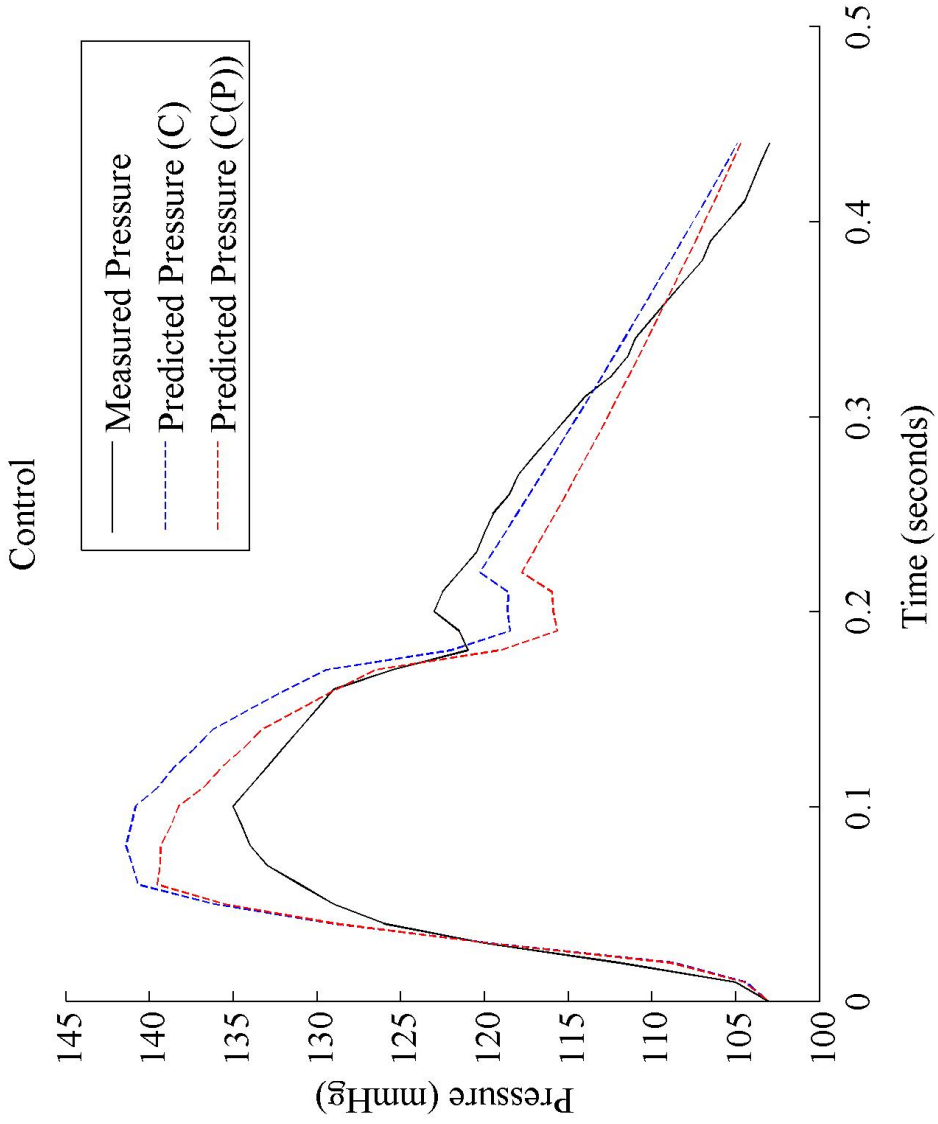

Figure 4.11: Predicted vs. measured pressure for control condition (dataset 5). Black solid line: measured pressure; blue dashed line: predicted pressure from linear compliance model; red dashed line: predicted pressure from non-linear compliance model.

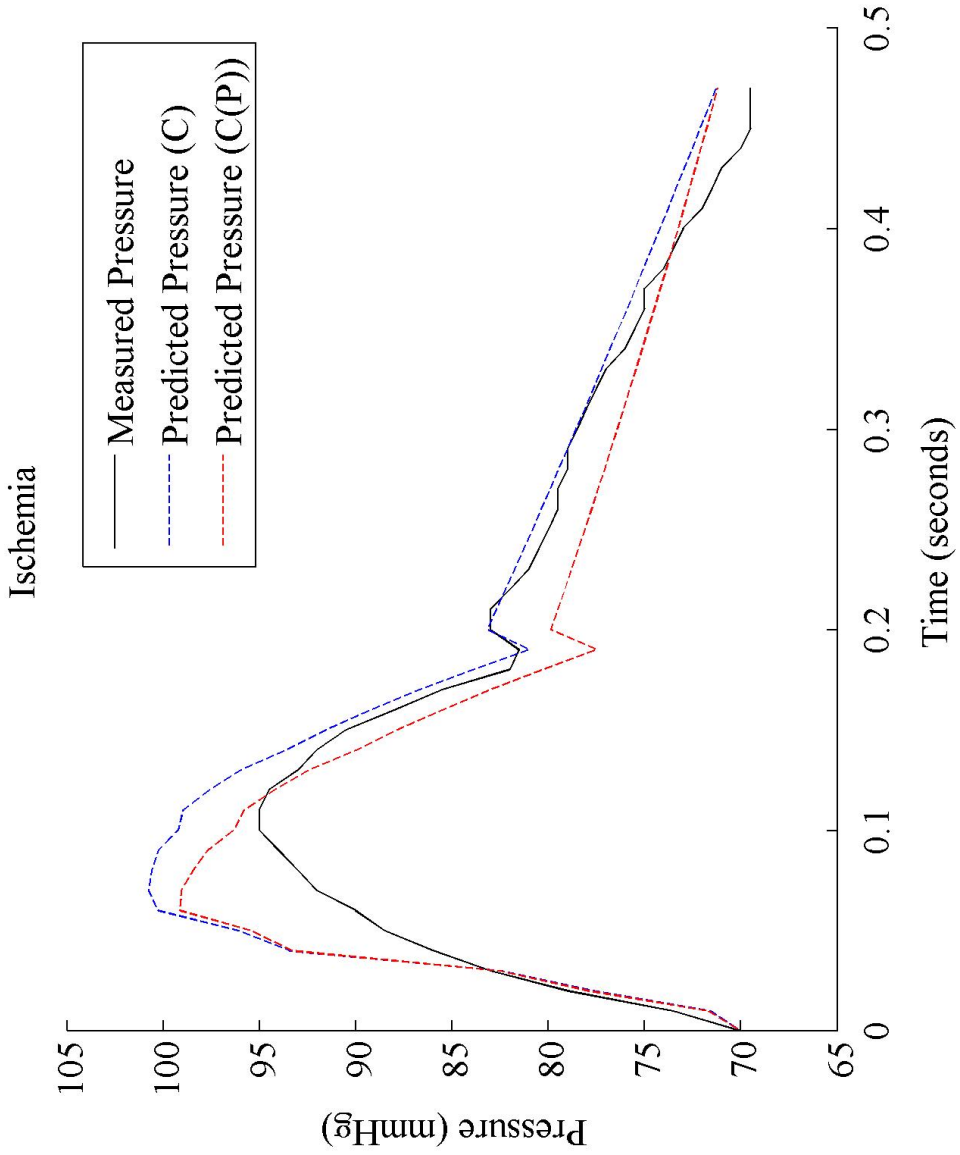

Figure 4.12: Predicted vs. measured pressure for ischemia condition (dataset 5). Black solid line: measured pressure; blue dashed line: predicted pressure from linear compliance model; red dashed line: predicted pressure from non-linear compliance model.

Dataset	Control		Hypertension		Vasodilation	
	C	C(P)	C	C(P)	C	C(P)
1	7.605	0.035	19.302	0.050	2.035	1.82E-04
2	20.392	5.092	29.001	0.258	13.271	7.180
3	2.741	0.005	-----	-----	2.611	2.64E-04
4	-----	-----	14.874	0.017	3.362	1.99E-04
Mean	10.246	1.711	21.059	0.108	6.223	2.394
St. Dev.	9.117	2.929	7.225	0.130	5.329	3.590

Table 4.3: Root mean square error between predicted pressure and compliance models (datasets 1-4). *"C"*: pressure-independent, linear compliance model; *"C(P)"*: pressure-dependent, non-linear compliance model. Compliance units: mL/mmHg.

Dataset	Control		Ischemia	
	C	C(P)	C	C(P)
5	11.148	0.049	13.084	0.034
6	2.164	0.010	5.175	0.009
7	0.867	0.001	6.090	0.013
Mean	4.726	0.020	8.116	0.019
St. Dev.	5.599	0.026	4.326	0.014

Table 4.4: Root mean square error between predicted pressure and compliance models (datasets 5-7). *"C"*: pressure-independent, linear compliance model; *"C(P)"*: pressure-dependent, non-linear compliance model. Compliance units: mL/mmHg.

The second type of plot compares the non-linear compliance with the measured pressure wave. Both parameters were plotted against time in order to compare the relationship between the model-based arterial compliance and pressure for a complete cardiac cycle (systolic and diastolic). Figures 4.13-4.15 present the described relationship for control, hypertension, and vasodilation and figures 4.16 and 4.17 are plots for control and ischemia. In all cases, compliance maintains a value close to its maximum in early systole. During mid-systole the compliance begins to decline until reaching its minimum in late systole. During the diastolic phase the compliance steadily increases towards its maximum.

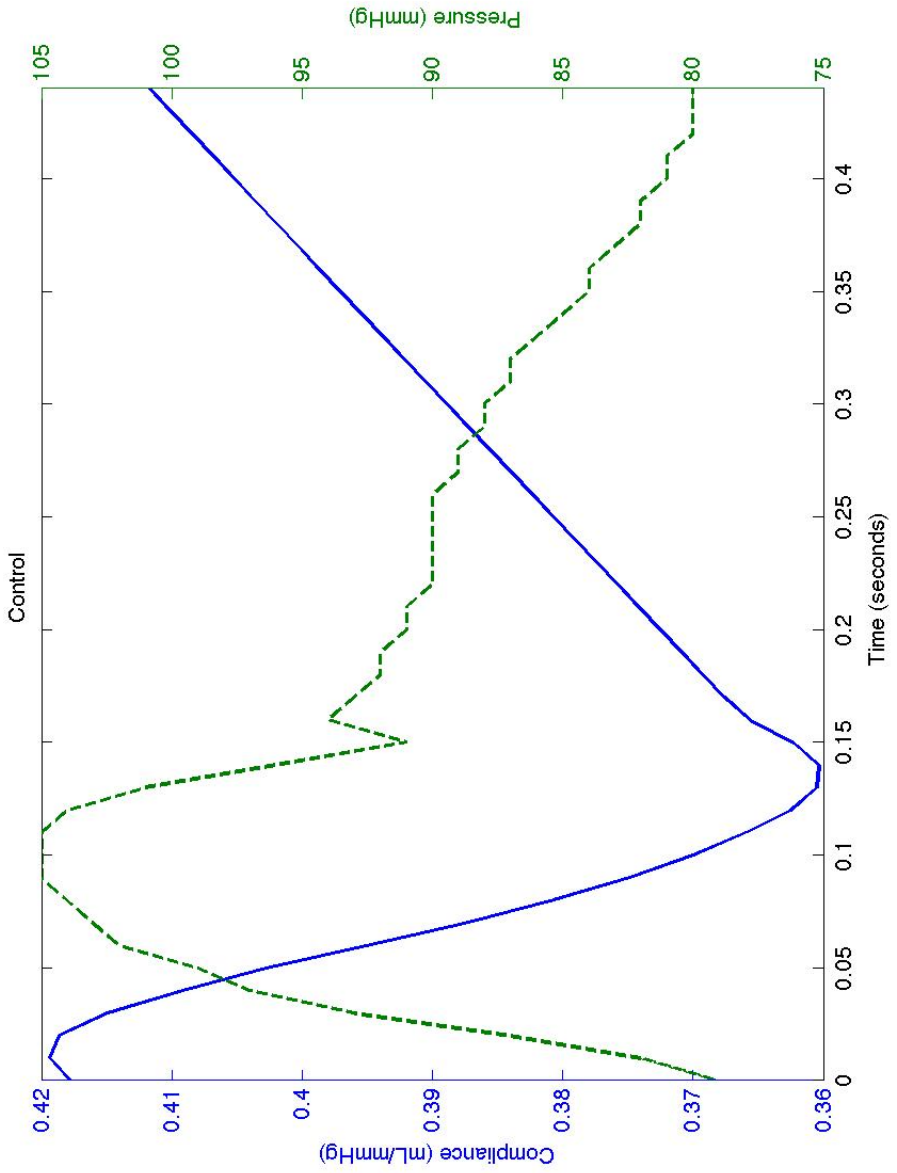

Figure 4.13: Compliance and pressure versus time for control condition (dataset 1).

Blue line: non-linear compliance; green dotted line: pressure waveform.

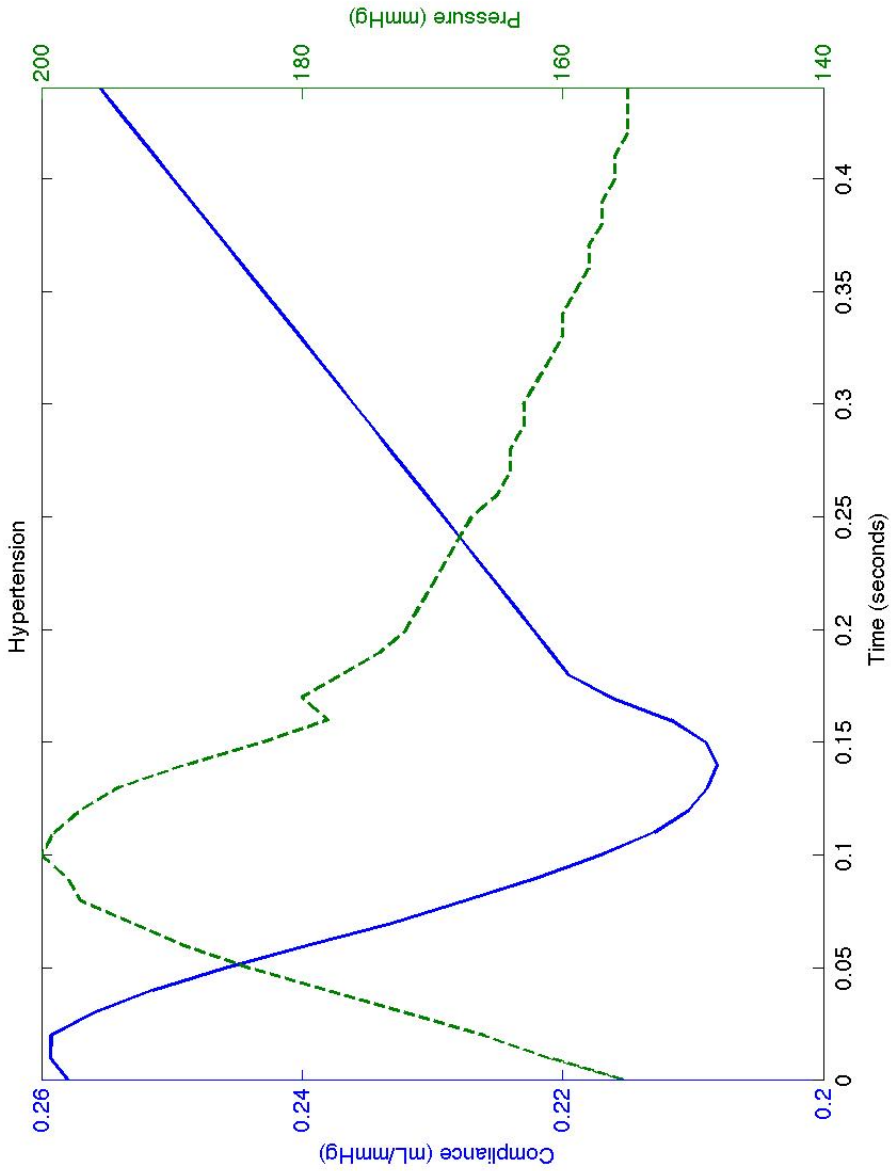

Figure 4.14: Compliance and pressure versus time for hypertension condition (dataset 1). Blue line: non-linear compliance; green dotted line: pressure waveform.

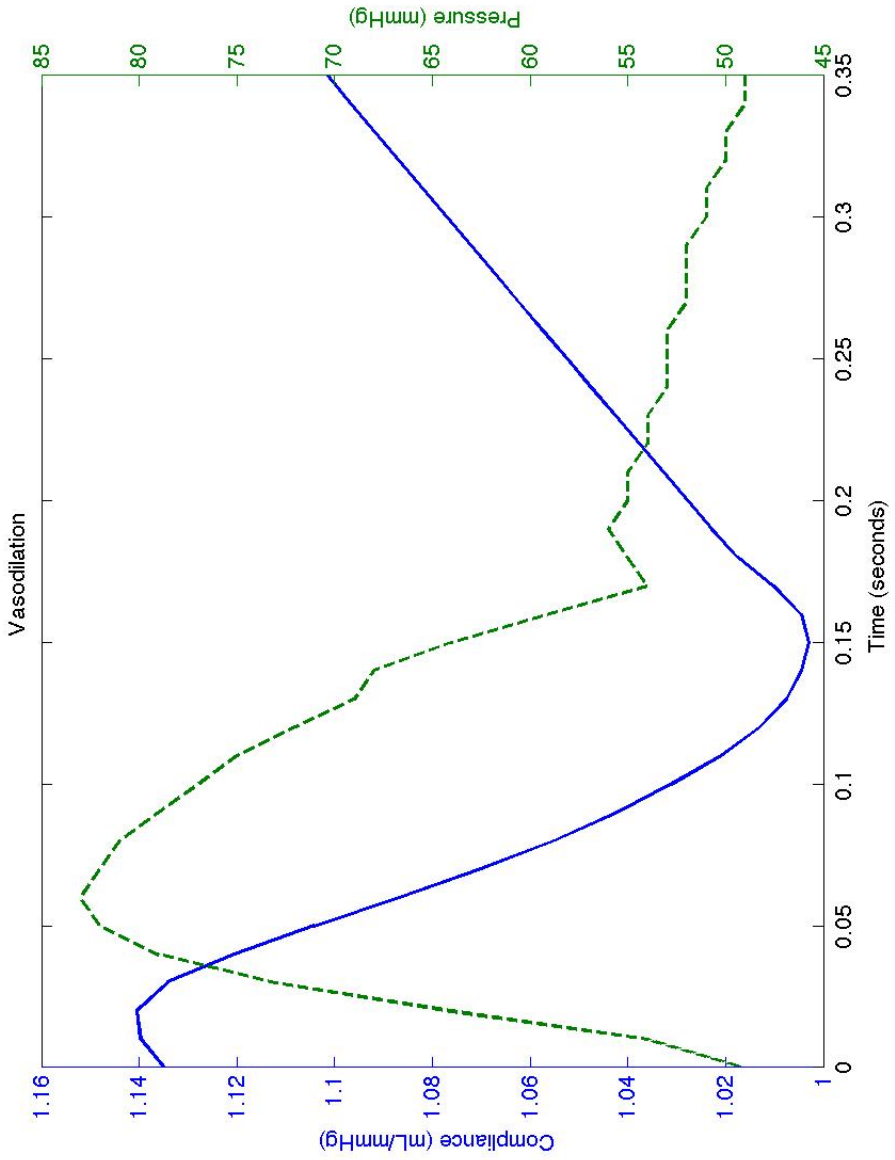

Figure 4.15: Compliance and pressure versus time for vasodilation condition (dataset 1). Blue line: non-linear compliance; green dotted line: pressure waveform.

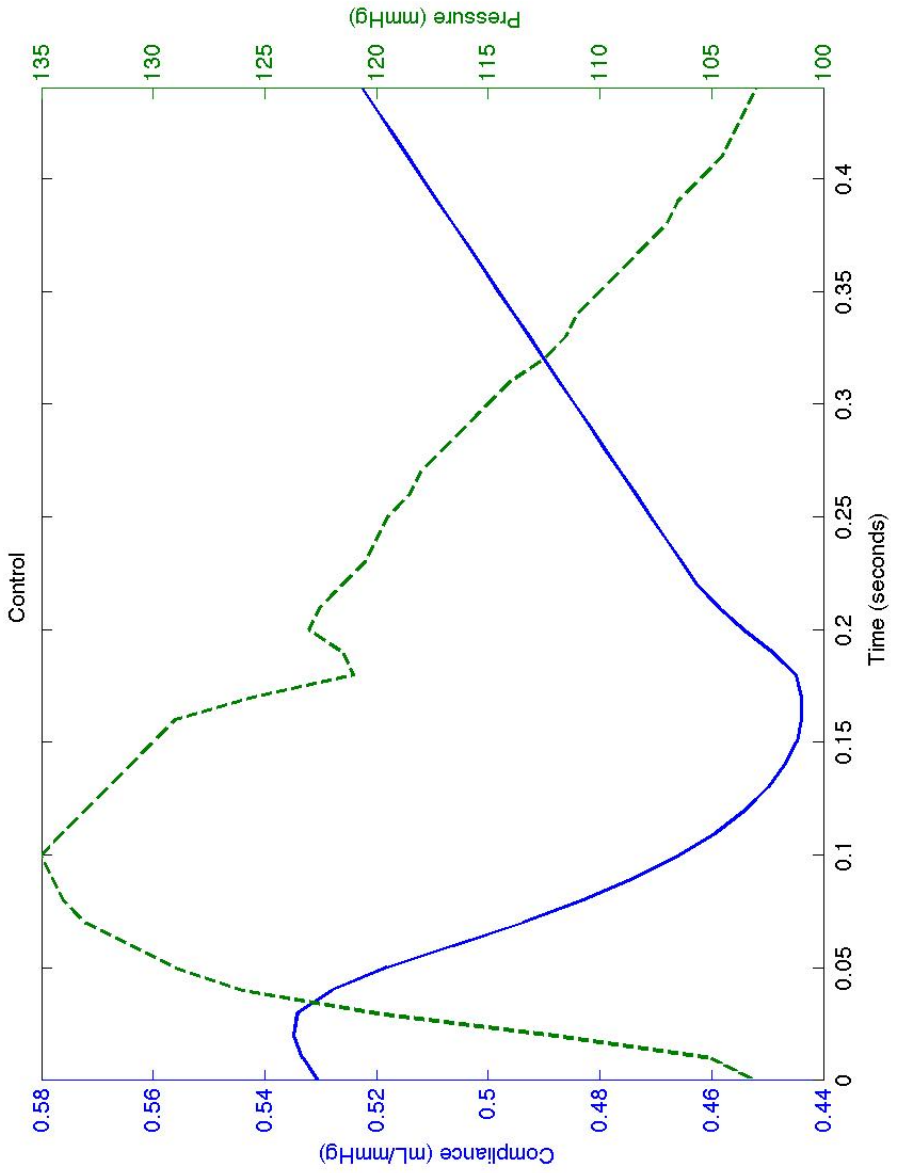

Figure 4.16: Compliance and pressure versus time for control condition (dataset 5).

Blue line: non-linear compliance; green dotted line: pressure waveform.

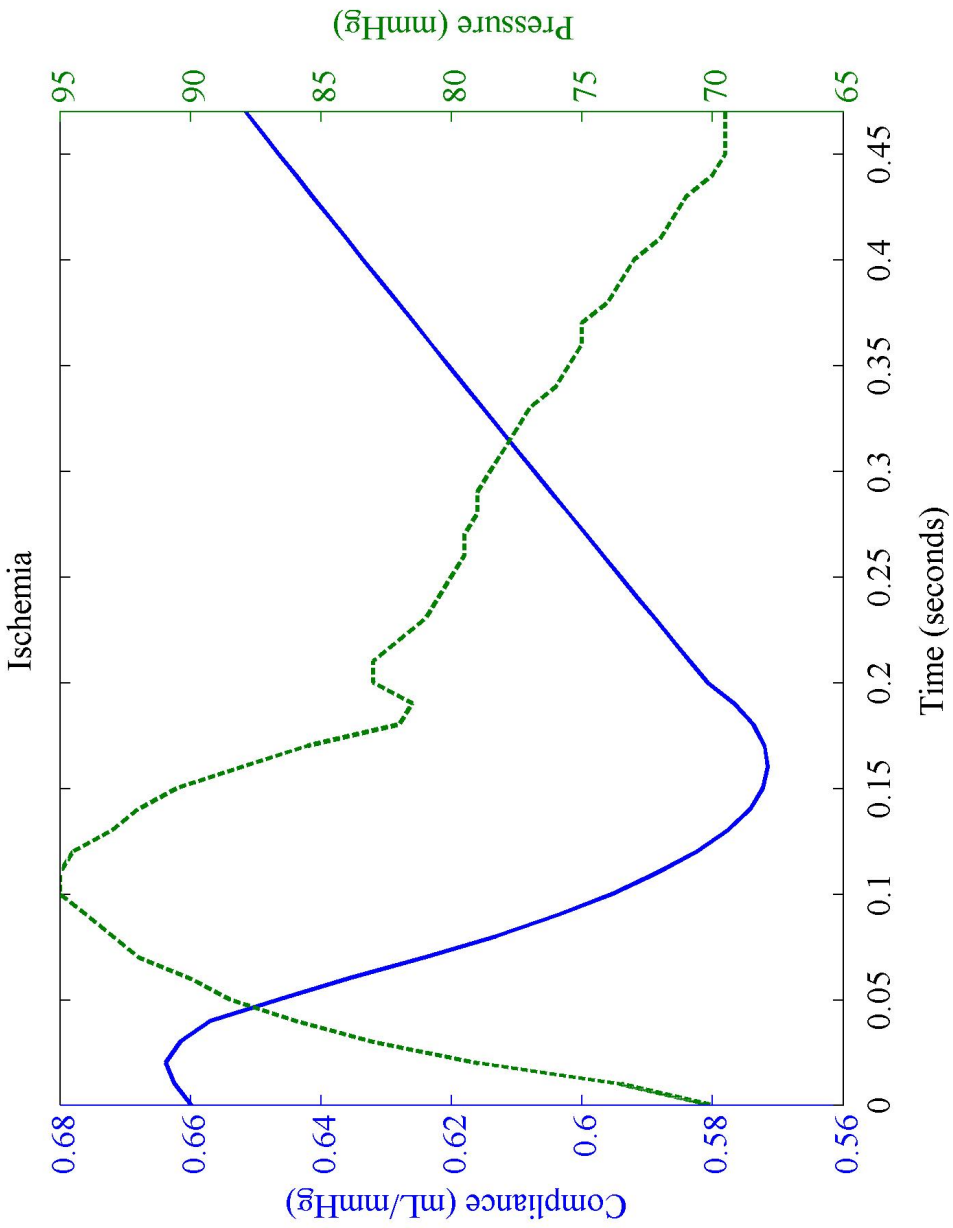

Figure 4.17: Compliance and pressure versus time for ischemia condition (dataset 5). Blue line: non-linear compliance; green dotted line: pressure waveform.

The third type of plot shows the non-linear compliance as a function of pressure. The compliance was plotted against pressure to generate compliance-pressure loops. Figures 4.18 and 4.19 show the compliance-pressure loops for control, hypertension, and vasodilation. The loop for the hypertension condition indicates a lower overall compliance as well as a smaller range compared to the control condition. The vasodilation loop indicates a higher overall compliance and a larger range compared to the control condition. Figures 4.20 and 4.21 show the loops for control and ischemia. The compliance-pressure loop for the ischemia condition indicates a higher overall compliance.

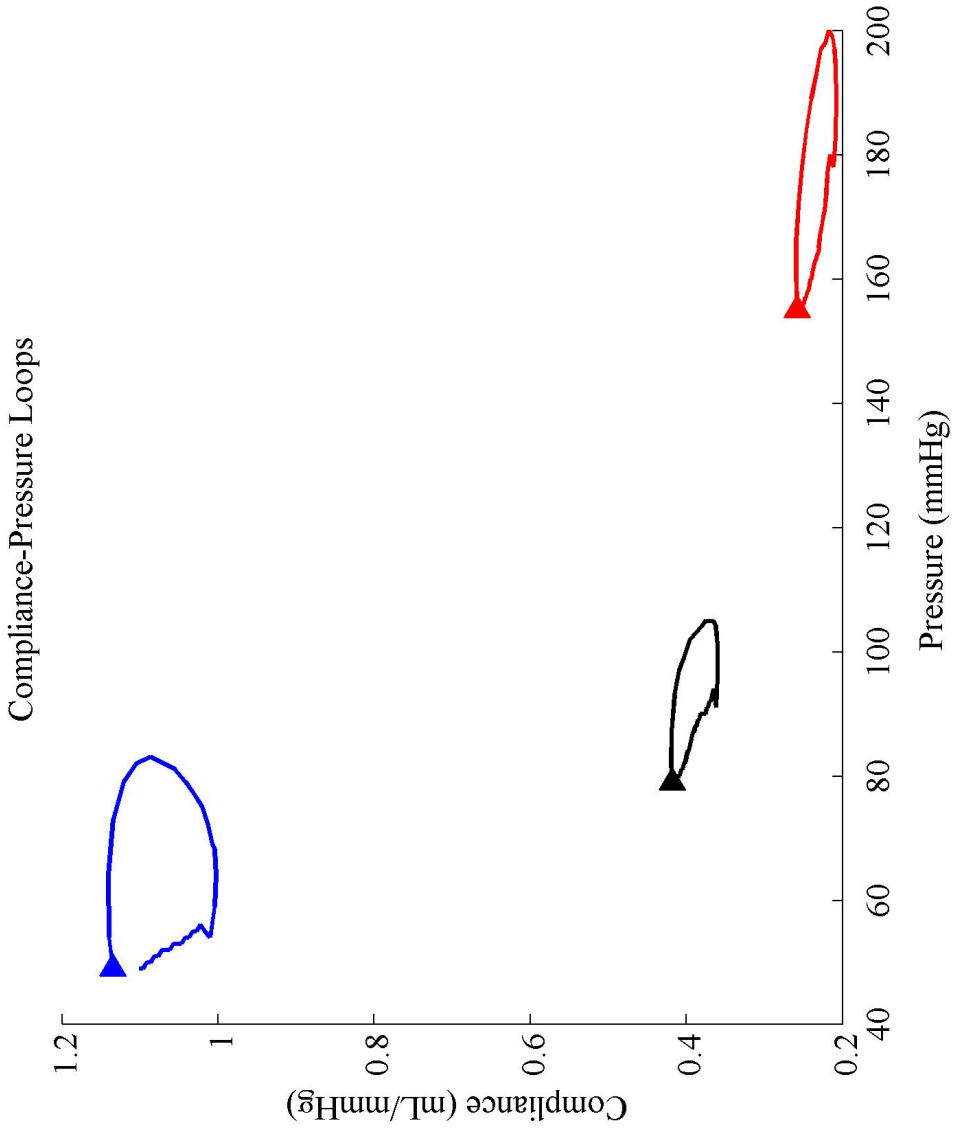

Figure 4.18: Compliance-Pressure loops (dataset 1). Black line: control condition; red line: hypertension condition; blue line: vasodilation condition.

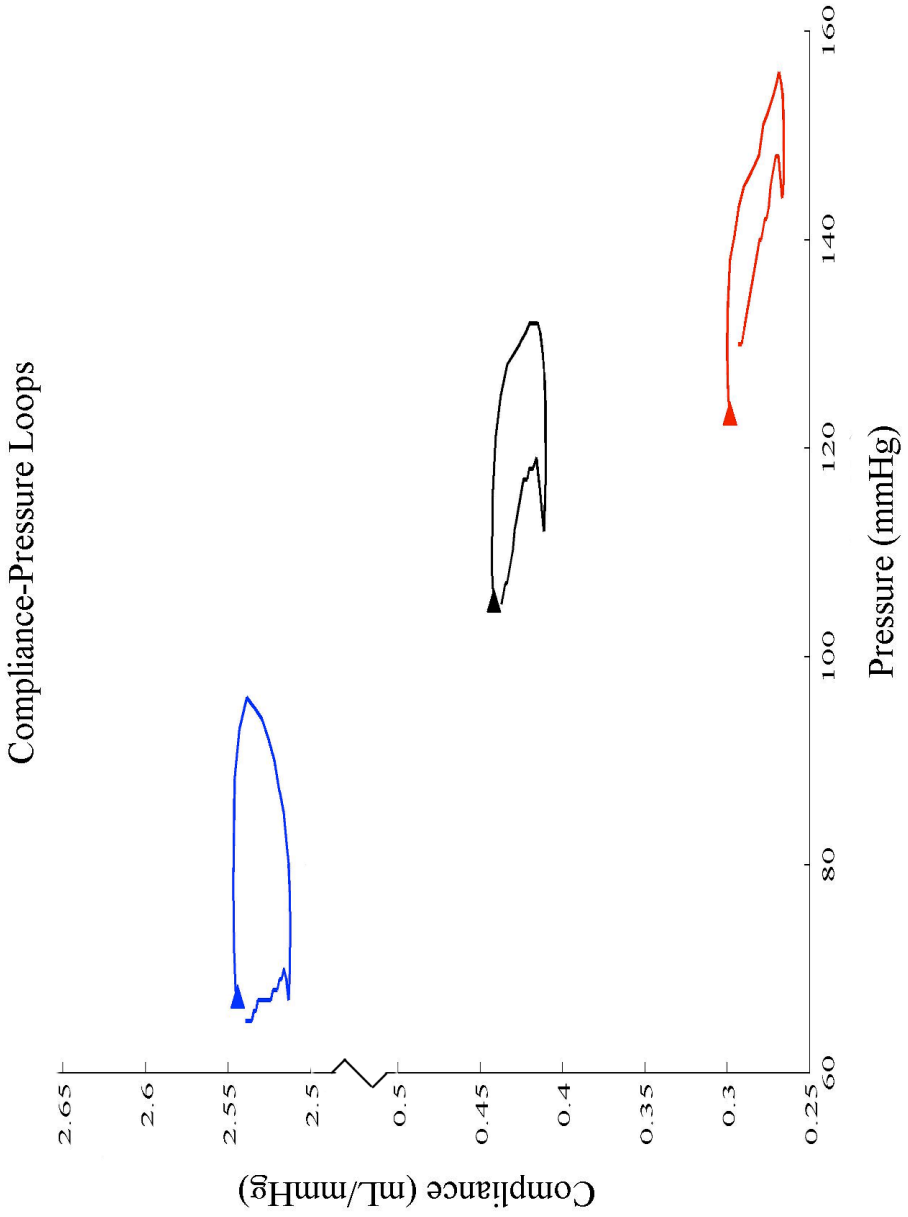

Figure 4.19: Compliance-Pressure loops (dataset 2). Black line: control condition; red line: hypertension condition; blue line: vasodilation condition.

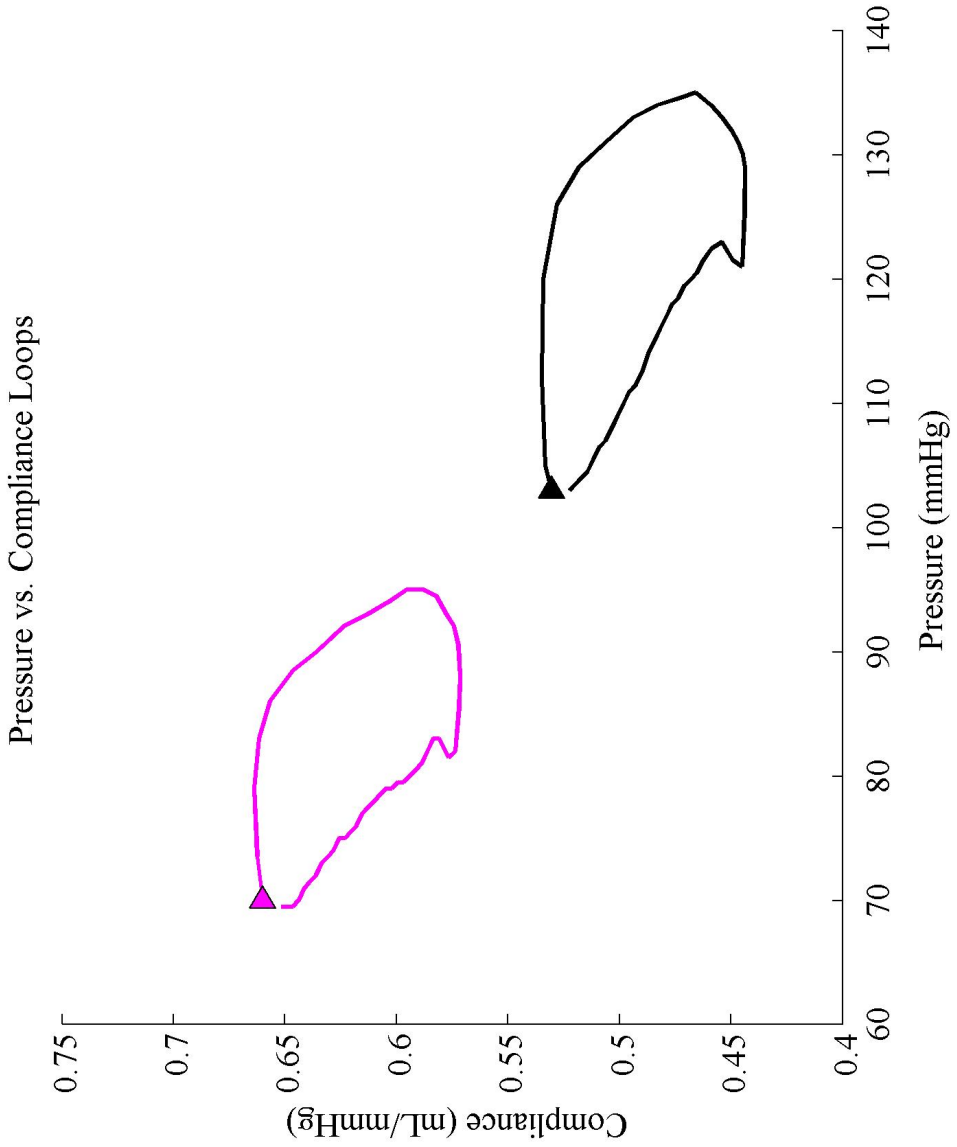

Figure 4.20: Compliance-Pressure loops (dataset 5). Black line: control condition; pink line: ischemia condition.

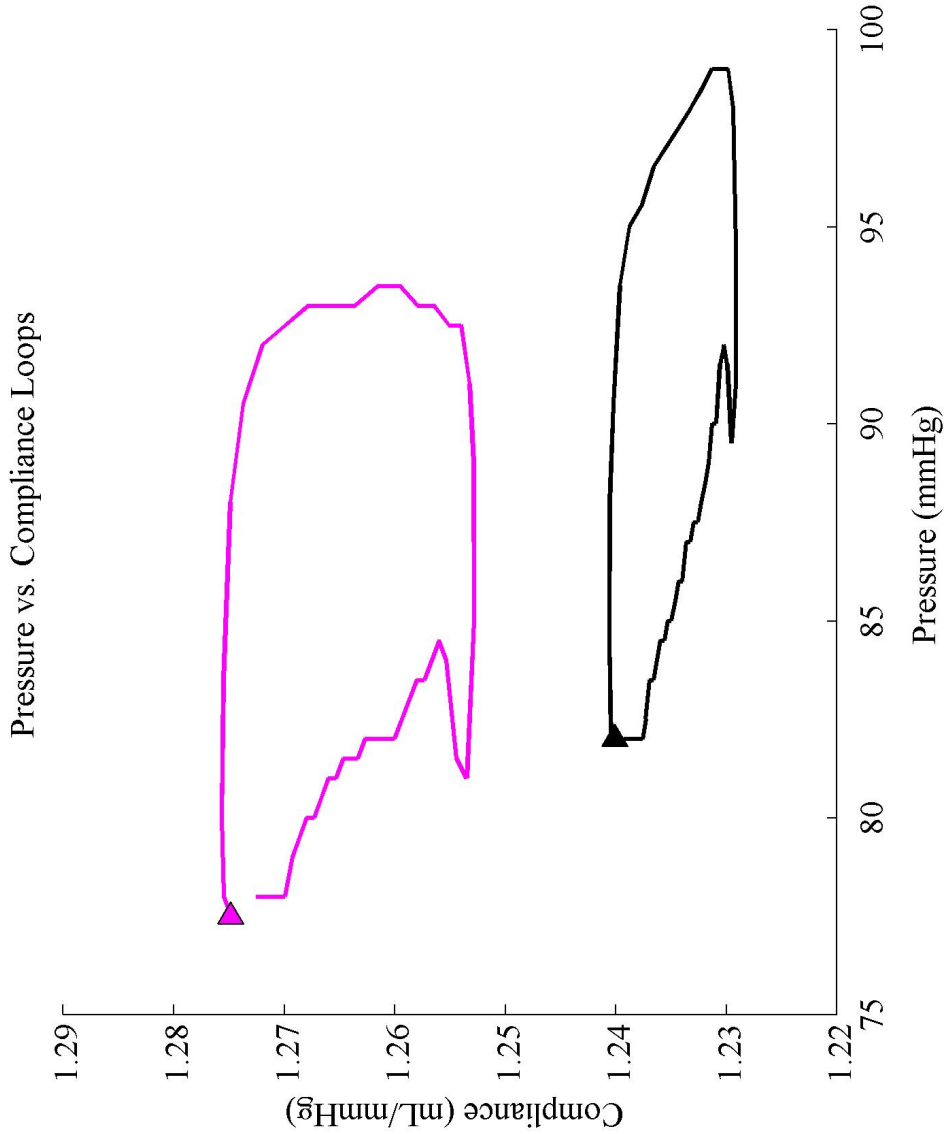

Figure 4.21: Compliance-Pressure loops (dataset 7). Black line: control condition; pink line: ischemia condition.

The numerical values of the Windkessel parameters for all the datasets are presented in tables 4.5 and 4.6.

Dataset	Characteristic Impedance (Z_0)			Peripheral Resistance (R_s)			Compliance (C)		
	Control	MTX	NTP	Control	MTX	NTP	Control	MTX	NTP
1	0.190	0.340	0.255	4.670	10.677	1.852	0.482	0.190	1.000
2	0.205	0.191	0.195	4.851	4.988	2.136	0.671	0.451	1.568
3	0.243	-----	0.168	5.947	-----	2.671	0.443	-----	1.235
4	-----	0.219	0.174	-----	6.424	2.932	-----	0.296	1.542
Mean	0.213	0.250	0.198	5.156	7.363	2.398	0.532	0.312	1.336
St. Dev.	0.028	0.079	0.040	0.691	2.958	0.492	0.122	0.131	0.270

Table 4.5: Characteristic impedance, peripheral resistance, and linear compliance (datasets 1-4). *"MTX"*: hypertension condition; *"NTP"*: vasodilation condition.

Dataset	Characteristic Impedance (Z_0)		Peripheral Resistance (R_s)		Compliance (C)	
	Control	I	Control	I	Control	I
5	0.198	0.245	3.826	3.840	0.422	0.458
6	0.218	0.275	3.080	4.444	0.711	0.729
7	0.078	0.099	2.595	2.697	1.277	1.671
Mean	0.165	0.206	3.167	3.660	0.803	0.953
St. Dev.	0.075	0.094	0.620	0.887	0.435	0.637

Table 4.6: Characteristic impedance, peripheral resistance, and linear compliance (datasets 5-7). *"I"*: ischemia condition.

4.3. Augmentation Indices

The results from the augmentation index calculations are presented in tables 4.7 and 4.8. In order to determine if each augmentation index calculation could be used to distinguish between the conditions, ANOVA statistical tests were performed. The significance test compared the control, hypertension, and vasodilaton conditions or the control and ischemia conditions for each augmentation index. The null hypothesis was that the mean augmentation index for each condition did not differ from each other. If the p-value obtained from the statistical tests is below the chosen significance level ($p<0.01$), then the null hypothesis is rejected. A rejected hypothesis indicates the differences between the mean values are significant and the conclusion can be drawn that the augmentation index calculation is a good method to distinguish between the conditions.

In table 4.7, The ANOVA tests for all five augmentation index calculations resulted in p-values less than the significance level. The results indicate that each calculation method can distinguish between the control, hypertension, and vasodilation conditions. Conversely, the ANOVA tests for the data in table 4.8 resulted in p-values greater than the significance level. These results indicate that none of the calculation methods are able to distinguish between the control and ischemia conditions.

Dataset	AIx_1			AIx_2			AIx_3			AIx_4			AIx_5		
	Control	MTX	NTP	Control	MTX	NTP	Control	MTX	NTP	Control	MTX	NTP	Control	MTX	NTP
1	0.173	0.244	0.029	0.798	0.852	0.524	0.681	0.755	0.448	0.759	0.793	0.448	0.045	0.058	0.012
2	0.204	0.333	0.000	0.806	0.905	0.562	0.731	0.800	0.529	0.794	0.863	0.529	0.044	0.076	0.000
3	0.083	-----	0.000	0.796	-----	0.677	0.675	-----	0.615	0.734	-----	0.615	0.018	-----	0.000
4	-----	0.255	0.000	-----	0.900	0.675	-----	0.817	0.620	-----	0.852	0.620	-----	0.054	0.000
Mean	0.153	0.277	0.007	0.800	0.886	0.610	0.696	0.791	0.553	0.762	0.836	0.553	0.036	0.063	0.003
St. Dev.	0.063	0.049	0.015	0.005	0.029	0.078	0.030	0.032	0.082	0.030	0.038	0.082	0.015	0.012	0.006
ANOVA (p-value)	2.587E-04			6.845E-04			3.100E-03			9.761E-04			6.089E-04		

Table 4.7: Augmentation Indices (datasets 1-4). The results of the ANOVA statistical tests are shown as well (p-values). *"MTX"*: hypertension condition; *"NTP"*: vasodilation condition.

Dataset	AIx_1		AIx_2		AIx_3		AIx_4		AIx_5	
	Control	I	Control	I	Control	I	Control	I	Control	I
5	0.125	0.200	0.781	0.722	0.610	0.573	0.726	0.673	0.031	0.056
6	0.023	0.079	0.709	0.773	0.591	0.616	0.669	0.664	0.006	0.018
7	0.118	0.031	0.858	0.817	0.793	0.763	0.832	0.781	0.021	0.005
Mean	0.089	0.103	0.783	0.771	0.665	0.651	0.742	0.706	0.019	0.026
St. Dev.	0.057	0.087	0.075	0.048	0.111	0.099	0.083	0.065	0.013	0.026
ANOVA (p-value)	8.192E-01		8.256E-01		8.791E-01		5.822E-01		7.006E-01	

Table 4.8: Augmentation Indices (datasets 5-7). The results of the ANOVA statistical tests are shown as well (p-values). *"I"*: ischemia condition.

Chapter 5: Discussion and Future Research

5.1. Pressure and Flow Comparisons

The results showed significant changes in the arterial pressure and blood flow between control, hypertension, vasodilation, and ischemia. Hypertension is generally associated with increased vascular resistance or increased stroke volume. The vascular resistance is determined by the vascular tone or constriction of the blood vessels (Bohr, et. al. 1984). The administration of methoxamine in the dogs induced vasoconstriction of the blood vessels and simulated the effects of hypertension. The vasoconstriction, or narrowing of the blood vessels, causes an increase in resistance leading to increased arterial pressure as demonstrated by the results (figure 4.2). Additionally, the increased resistance causes an increase in the ratio of peak reflected pressure to peak forward pressure (table 4.1). Both the forward and reflected pressure waves will increase due to the increase in overall pressure. However, the reflected wave will increase by a greater percentage since the narrowed blood vessels and increased resistance will directly interfere with the blood flow progression (figure 4.6) and greatly increase the reflected pressure wave.

The administration of sodium nitroprusside induced vasodilation of the blood vessels. The increase in blood vessel diameter will reduce the arterial resistance leading to a decrease in pressure (figure 4.3). The decreased resistance causes a decrease in the ratio of peak reflected pressure to peak forward pressure (table 4.1). The widening of the blood vessels and reduced resistance allows the blood to flow easily (figure 4.6) and

generates a large forward pressure wave. The reflected wave will be small since there is little interference with the blood flow progression.

The mechanical occlusion of the left anterior descending coronary artery simulated the effect of myocardial ischemia. The occlusion causes a decrease in cardiac output leading to decreased blood flow (figure 4.7). The reduced blood flow results in less blood flowing through the blood vessels, which corresponds to the decrease in pressure that is observed (figure 4.5). Since the overall pressure decreases, the peak forward and peak reflected pressure values also decrease (table 4.2). However, the mechanical occlusion of the coronary artery does not alter the blood vessels' structure (i.e. no vasoconstriction or vasodilation), so beyond the site of occlusion the blood can flow unimpeded and there is no significant change in the ratio of peak forward to peak reflected pressure.

5.2. Compliance Comparisons

The three-element Windkessel model was implemented using the common linear, pressure-independent compliance method and the nonlinear, pressure-dependent compliance method. The plots comparing the measured pressure with the predicted pressures from each method (figures 4.8-4.12) demonstrated that utilization of a nonlinear compliance parameter produces a more accurate Windkessel model. This conclusion is corroborated by the root mean square error analysis (tables 4.3 and 4.4). The root mean square error value represents the variation of the predicted pressure curve from the measured pressure curve. The predicted pressure curves generated from the nonlinear Windkessel models produced lower errors indicating better predictions.

Once it was determined that nonlinear compliance produced a more accurate model than linear compliance, the changes in compliance throughout the cardiac cycle were compared to the changes in pressure (figures 4.13-4.17). Arterial compliance is largest during early systole, despite changes in pressure and flow. The high compliance facilitates left ventricular ejection of blood into the arteries. The decline of compliance during mid-systole corresponds with reduced ventricular ejection and increased arterial pressure caused by blood flowing into the arteries. In late-systole, as the arterial flow and pressure decline, the compliance continues to decline and is lowest at end systole. In the diastolic phase when aortic blood flow is zero, due to no ventricular ejection (figures 4.6 and 4.7), the compliance follows the exponential relationship described by equation 1.3.5 and increases towards its maximum.

The compliance-pressure loops (figures 4.18-4.21) present an alternative visual to the relationship between compliance and pressure. Recall that compliance is the ratio of the change in blood volume to the change in blood pressure (equation 1.3.3) and represents the ability of a blood vessel to resist recoil to its original dimensions. The position of the loops in comparison to the control shows that hypertension causes lower compliance, while vasodilation and ischemia leads to higher compliance. During hypertension, the blood vessels are constricted and cannot be easily stretched. The vasoconstriction causes arterial stiffness and does not allow the blood vessel to expand. The lack of flexibility leads to a high recoil force and blood vessels with low compliance. This corresponds with equation 1.3.3, since in hypertension blood flow decreases and pressure increases. Vasodilated blood vessels are easily stretched, have an increased diameter, and are flexible. In addition to the low recoil force, blood flow increases and

pressure decreases leading to a high compliance. Under ischemic conditions the blood flow and pressure in the blood vessels are decreased, which corresponds to only minor changes in compliance. If the compliance remains unchanged while both blood flow and pressure are reduced, there will be a significant decrease in blood delivered to the organs and tissues. However, the results show a distinctive increase in compliance during ischemia. This indicates the presence of a compensating mechanism to increase blood vessel compliance under ischemic conditions in order to maintain blood delivery throughout the body.

The shape of each loop provides further indication of arterial stiffness. Compared to the control loop, the hypertension loop yields a more oblong narrow shape, the vasodilation loop has a more circular shape, and the ischemia loop remains relatively unchanged. The narrow and oblong shape exhibited by the hypertension loop corresponds to a small compliance range. This indicates that the blood vessel cannot expand and has increased arterial stiffness. The more circular shape, exhibited in vasodilation, corresponds to a large compliance range indicating high flexibility and low arterial stiffness. The unchanged ischemia loop indicates no change in arterial stiffness. Since myocardial ischemia is generally caused by a local occlusion of a blood vessel, there is no overall physical change to the blood vessel structure.

5.3. Augmentation Index Comparisons

The current method of augmentation index calculation (equation 3.4.1) was compared to four experimental calculation methods (equations 3.4.2-3.4.5). An ANOVA statistical comparison of the results determined that each calculation method produced a

significant variation between control, hypertension, and vasodilation. Based on the p-values, the current method of augmentation index calculation (AIx_1) yielded the most statistically significant variation and should still be considered the best method. AIx_5 would be the next best method, followed by AIx_2, AIx_4, and AIx_3. However, further examination of the data in table 4.7 indicates potential flaws in the equations for AIx_1 and AIx_5 (equations 3.4.1 and 3.4.5).

Both methods rely on the relationship between systolic pressure and inflection pressure. Recall, that the inflection pressure represents the initial upstroke of the reflected pressure wave (O'Rourke, et. al. 2010). The inherent difficulty in calculating this value can lead to discrepancies. For the calculations in this thesis, the inflection pressure was recorded as the measured pressure at peak blood flow. In the vasodilation condition, datasets 2, 3, and 4 resulted in inflection pressures equivalent to systolic pressures. Since the parameters were equivalent, the values for AIx_1 and AIx_5 were zero. The zero values do not provide reliable insight into the measure of arterial stiffness. One possible solution is to use a more accurate method for the calculation of inflection pressure. However, the alternative methods are significantly more difficult and time consuming to calculate making their use impractical for clinical settings. The other experimental calculations, AIx_2, AIx_3, and AIx_4, do not suffer from this issue and are potentially better indicators of hypertension than the current method.

The ANOVA statistical comparison also showed that there was no significant variation between control and ischemia for any of the augmentation index calculations (table 4.8). Recall, from sections 5.1 and 5.2, that there is no significant change in arterial stiffness or the ratio of forward to reflected pressure between the control and ischemia

conditions. Since augmentation index is a measure of arterial stiffness and is dependent upon the relationship between the pressure pulse wave, forward pressure wave, and reflected pressure wave, this result coincides with the previous findings. While augmentation index is a good indicator of hypertension, it cannot be used for ischemia.

5.4. Further Research

The results presented demonstrate the accuracy and usefulness of the nonlinear three-element Windkessel model in representing the arterial system. While previous studies (Segers, et. al. 2005, Westerhof, et. al. 2008) have indicated that the linear four-element Windkessel model provides only a minimal increase in accuracy, further investigation utilizing pressure-dependent compliance should be conducted. The improved accuracy of the nonlinear four-element Windkessel model may be significant enough to warrant examination of improved inertance estimation methods.

The compliance-pressure loops showed significant change in arterial compliance in hypertension and ischemia. Compliance is affected by changes in blood flow, blood pressure, and peripheral resistance, making it an important cardiovascular parameter. Calculation of pressure-dependent compliance for other cardiovascular disorders is necessary to further understand the relationship between compliance and cardiac events.

Augmentation index proved to be a good indicator of hypertension, but not ischemia. The specificity of augmentation index prevents it from being a good indicator of disorders that do not directly affect arterial stiffness. Hypertension is a major risk factor for many other cardiovascular disorders, such as stroke and myocardial infarction. The different augmentation index calculations should be tested for the other major

cardiovascular disorders. If the results are similar to the ischemia data, augmentation index cannot be considered the best parameter to reflect general cardiovascular function. Future investigation should focus on developing a cardiovascular parameter that can distinguish between the various cardiovascular disorders. The ideal parameter should be able to determine the cause of hypertension or predict the risk of future cardiac events.

Due to the complexity of the cardiovascular system, a single parameter is unlikely to provide the required information for cardiovascular risk. However, a combination of easily derived parameters such as pressure-dependent compliance and augmentation index may be sufficient.

APPENDIX I: MATLAB Code

```
% Main Program

clear all
close all

n = '1';    % C,H,V Worksheet to Load: '1', '2', '3', or '4'
DoPlots = 0; % 1 = Plots On, 0 = Plots off
ni = '5';   % I Worksheet to Load: '5', '6', or '7'

% Load Data from excel file
    data = xlsread('MatlabData.xls',n);
    t = data(:,1);      % Time (seconds)
    C = data(:,2:3);    % Control (CMTX), Column 1: Pressure (P),
                        % Column 2: Flow (Q)
    H = data(:,4:5);    % Hypertension (MTX), Column 1: Pressure (P),
                        % Column 2: Flow (Q)
    V = data(:,6:7);    % Vasodilation (NTP), Column 1: Pressure (P),
                        % Column 2: Flow (Q)

    datai = xlsread('MatlabData.xls',ni);
    ti = datai(:,1);   % Time (seconds)
    Ci = datai(:,2:3); % Control, Col 1: Pressure (P), Col 2: Flow (Q)
    I = datai(:,4:5);  % Ischemia, Col 1: Pressure (P), Col 2: Flow (Q)

    % Remove NaN values
        C(any(isnan(C),2),:) = []; H(any(isnan(H),2),:) = [];
        V(any(isnan(V),2),:) = [];
        Ci(any(isnan(Ci),2),:) = []; I(any(isnan(I),2),:) = [];

% Estimate End Systolic Pressure
    if n == '1'
        PesC = 91; PesH = 178; PesV = 54;
    elseif n == '2'
        PesC = 112; PesH = 144; PesV = 69;
    elseif n == '3'
        PesC = 102; PesH = 3; PesV = 59.5;
    elseif n == '4'
        PesC = 3; PesH = 167.6; PesV = 83.2;
    end

    if ni == '5'
        PesCi = 121; PesI = 81.5;
    elseif ni == '6'
        PesCi = 76; PesI = 73;
    elseif ni == '7'
        PesCi = 89.5; PesI = 83;
    elseif ni == '8'
        PesCi = 84.5; PesI = 86;
    elseif ni == '9'
        PesCi = 99.5; PesI = 81;
    elseif ni == '10'
        PesCi = 76; PesI = 76;
    end
```

```
% Calculate Z values
    ZC = CalcZ(C); ZH = CalcZ(H); ZV = CalcZ(V);
    ZCi = CalcZ(Ci); ZI = CalcZ(I);

% Calculate Forward and Reflected Pressure waves
    % Forward Waves
        C(:,3) = 0.5.*(C(:,1) + (C(:,2).*ZC));
        H(:,3) = 0.5.*(H(:,1) + (H(:,2).*ZH));
        V(:,3) = 0.5.*(V(:,1) + (V(:,2).*ZV));
        Ci(:,3) = 0.5.*(Ci(:,1) + (Ci(:,2).*ZCi));
        I(:,3) = 0.5.*(I(:,1) + (I(:,2).*ZI));

    % Reflected Waves
        C(:,4) = 0.5.*(C(:,1) - (C(:,2).*ZC));
        H(:,4) = 0.5.*(H(:,1) - (H(:,2).*ZH));
        V(:,4) = 0.5.*(V(:,1) - (V(:,2).*ZV));
        Ci(:,4) = 0.5.*(Ci(:,1) - (Ci(:,2).*ZCi));
        I(:,4) = 0.5.*(I(:,1) - (I(:,2).*ZI));

% Calculate Augmentation Index
    AIxC = CalcAIx(C);
    AIxH = CalcAIx(H);
    AIxV = CalcAIx(V);
    AIxCi = CalcAIx(Ci);
    AIxI = CalcAIx(I);

if DoPlots == 1
% Plot Pressure Waves
    PlotPressure(t,C,'Control');
    PlotPressure(t,H,'Hypertensive');
    PlotPressure(t,V,'Vasodilated');
    PlotPressure(ti,Ci,'Control');
    PlotPressure(ti,I,'Ischemia');

% Comparison Plots
    PlotAllWaves(t,C(:,2),H(:,2),V(:,2),'Flow (mL / s)');
    PlotAllWavesI(ti,Ci(:,2),I(:,2),'Flow (mL/s)');
end

% Windkessel Model - to calculate Compliance (independent of pressure)
    CC = CalcC(t,C,PesC); CH = CalcC(t,H,PesH); CV = CalcC(t,V,PesV);
    CCi = CalcC(ti,Ci,PesCi); CI = CalcC(ti,I,PesI);

% Pressure Dependent Compliance
    CwaveC = CalcCwave(C,CC,ZC,'C'); CwaveH = CalcCwave(H,CH,ZH,'H');
    CwaveV = CalcCwave(V,CV,ZV,'V');
    CwaveCi = CalcCwave(Ci,CCi,ZCi,'Ci');
    CwaveI = CalcCwave(I,CI,ZI,'I');

if DoPlots == 1
% Plot Time vs. Compliance and Pressure
    PlotCvsT(t,C,CwaveC,'Control');
    PlotCvsT(t,H,CwaveH,'Hypertension');
    PlotCvsT(t,V,CwaveV,'Vasodilation');
    PlotCvsT(ti,Ci,CwaveCi,'Control');
```

```
    PlotCvsT(ti,I,CwaveI,'Ischemia');

% Plot Pressure vs. Compliance Comparisons
    PlotComparisonCvsP(C,H,V,CwaveC,CwaveH,CwaveV);
    PlotComparisonCvsPI(Ci,I,CwaveCi,CwaveI);

end

% Pressure predicted from Flow (using Rs and Compliance)
    PC = CalcP(C,CC,ZC);
    PH = CalcP(H,CH,ZH);
    PV = CalcP(V,CV,ZV);
    PCi = CalcP(Ci,CCi,ZCi);
    PI = CalcP(I,CI,ZI);

% Pressure predicted from Flow (using Rs and Pressure-dependent
Compliance)
    PdC = CalcPd(C,CwaveC,ZC);
    PdH = CalcPd(H,CwaveH,ZH);
    PdV = CalcPd(V,CwaveV,ZV);
    PdCi = CalcPd(Ci,CwaveCi,ZCi);
    PdI = CalcPd(I,CwaveI,ZI);

if DoPlots == 1

% Plot Measured Pressure vs. Predicted Pressure
    PlotPredPressures(t,C,PC,PdC,'Control');
    PlotPredPressures(t,H,PH,PdH,'Hypertension');
    PlotPredPressures(t,V,PV,PdV,'Vasodilation');
    PlotPredPressures(ti,Ci,PCi,PdCi,'Control');
    PlotPredPressures(ti,I,PI,PdI,'Ischemia');

end

%-------------------------------------------------------------------------
%-------------------------------------------------------------------------

function Z = CalcZ(d)

% Calculates the Z value of the data
% d(:,1) = Pressure values
% d(:,2) = Flow values

for x = 1:7
    zdata(x) = (d(x+1,1)-d(1,1)) / (d(x+1,2)-d(1,2));
end
Z = mean(zdata);

%-------------------------------------------------------------------------
%-------------------------------------------------------------------------

function AIx = CalcAIx(d)

% Calculates Augmentation Indexes (AIx1 - AIx5) of data
% Ps (Systolic Pressure) = maximum Pressure
```

```
% Pi (Inflection Pressure) = Pressure at maximum Flow
% Pd (Diastolic Pressure) = Pressure at time = 0
% Prp = Peak Reflected Pressure
% Pfp = Peak Forward Pressure
% PratPfpeak = Reflected Pressure at peak forward pressure
% PratPs = Reflected Pressure at Systolic Pressure
% PfatPs = Forward Pressure at Systolic Pressure

% Ps (Systolic Pressure) = maximum Pressure
[Ps Psi] = max(d(:,1));

% Pi (Inflection Pressure) = Pressure at maximum Flow
[r index] = max(d(:,2));
check = 0;
count = index;
while check == 0
    if d(count+1,2) == d(index,2)
        count = count + 1;
    else check = 1;
    end
end
Pi = mean(d(index:count,1));

% Pd (Diastolic Pressure) = Pressure at time = 0
Pd = d(1,1);

% Prp = Peak Reflected Pressure
[Prp Prpi] = max(d(:,4));

% Pfp = Peak Forward Pressure
[Pfp Pfpi] = max(d(:,3));

% PratPfpeak = Reflected Pressure at peak forward pressure
PratPfpeak = d(Pfpi,4);

% PratPs = Reflected Pressure at Systolic Pressure
PratPs = d(Psi,4);

% PfatPs = Forward Pressure at Systolic Pressure
PfatPs = d(Psi,3);

% Augmentation Index Calculations
AIx(1) = (Ps-Pi) / (Ps-Pd);
AIx(2) = Prp / Pfp;
AIx(3) = PratPfpeak / Pfp;
AIx(4) = PratPs / PfatPs;
AIx(5) = (Ps-Pi) / Pi;

%-------------------------------------------------------------------------
%-------------------------------------------------------------------------

function PlotPressure(t,d,cat)

% Plots the Total Pressure, Forward Pressure, and Reflected Pressure
% waves on the same plot
```

```
x = figure('name',[cat,' Pressure Wave Forms'],'numbertitle','off');
hold on;
[r c] = size(d);
plot(t(1:r),d(:,1),'-k','LineWidth',1.5);   % Total Pressure Wave
plot(t(1:r),d(:,3),'--k','LineWidth',1.5);  % Forward Pressure Wave
plot(t(1:r),d(:,4),':k','LineWidth',1.5);   % Reflected Pressure Wave
xlim([0,t(r)]); ylim([min(d(:,4))-5,max(d(:,1))+5]);
title(cat); xlabel('Time (seconds)'); ylabel('Pressure (mmHg)');
%legend('P_T', 'P_{forward}', 'P_{reflected}');
hold off;

%-----------------------------------------------------------------------
%-----------------------------------------------------------------------

function PlotAllWaves(t,c,h,v,cat)

% Plots comparisons of Control, Hypertensive, and Vasodilated wave
% forms
% c, h, and v are vectors containing the desired wave form values

x = figure('name',[cat,' Wave Forms'],'numbertitle','off');
hold on;
plot(t(1:length(c)),c,'k','LineWidth',1.5); % Control
plot(t(1:length(h)),h,'r','LineWidth',1.5); % Hypertensive
plot(t(1:length(v)),v,'b','LineWidth',1.5); % Vasodilated
test = [c; h; v];
low = min(min(test));
high = max(max(test));
xlim([0,t(end)]); ylim([low-5,high+5]);
title('Wave Comparison'); xlabel('Time (seconds)'); ylabel([cat]);
%legend('Control','Hypertensive','Vasodilated');
hold off;

%-----------------------------------------------------------------------
%-----------------------------------------------------------------------

function PlotAllWavesI(t,c,i,cat)

% Plots comparisons of Control and Ischemia wave forms
% c and i are vectors containing the desired wave form values

x = figure('name',[cat,' Wave Forms'],'numbertitle','off');
hold on;
plot(t(1:length(c)),c,'k','LineWidth',1.5); % Control
plot(t(1:length(i)),i,'m','LineWidth',1.5); % Ischemia
test = [c; i];
low = min(min(test));
high = max(max(test));
xlim([0,t(end)]); ylim([low-5,high+5]);
title('Wave Comparison'); xlabel('Time (seconds)'); ylabel([cat]);
%legend('Control','Ischemia');
hold off;

%-----------------------------------------------------------------------
%-----------------------------------------------------------------------
```

```
function C = CalcC(t,d,Pes)

% Calculate Compliance
% t = time
% d = data set
% Pes = Estimated End Systolic Pressure

Rs = mean(d(:,1)) / mean(d(:,2));   % Peripheral Resistance
Pd = d(end,1);                      % End Diastolic Pressure

[Ps Psi] = max(d(:,1));
count = Psi;
check = 0;
while check == 0
    if d(count+1,1) > d(count,1)
        check = 1;
    else count = count+1;
    end
end
[r c] = size(d);
td = t(r) - t(count);

C = -td / (log(Pd/Pes)*Rs);

%-------------------------------------------------------------------------
%-------------------------------------------------------------------------

function Cwave = CalcCwave(d,C,Z,cat)

% Calculates Pressure dependent Compliance wave
% d = data set
% C = compliance (independent of pressure)
% cat = 'C', 'H', 'V', or 'I'

% Parameters
    [a b] = abtest(d,C,Z,cat);
    dt = 0.01;  % sampling interval (10 msec)
    Rs = mean(d(:,1)) / mean(d(:,2));   % Peripheral Resistance

% Calculate Pt
Pt(1) = d(1,1);  % Initial Pressure (measured)
for x = 1:length(d(:,1))-1
    Pt(x+1) = Pt(x) + dt.*(d(x,2)-Pt(x)./Rs)./C;
end

% Calculate Compliance
Cwave = a.*exp(b.*Pt(:));

%-------------------------------------------------------------------------
%-------------------------------------------------------------------------

function PlotCvsT(t,d,Cwave,cat)

% Plot Compliance and Pressure vs. Time
```

```
% t = time
% d = data set
% Cwave = compliance wave

x = figure('name','Compliance & Pressure vs.Time','numbertitle','off');
hold on;
[r c] = size(d);

[ax,h1,h2] = plotyy(t(1:r),Cwave,t(1:r),d(:,1));
title([cat]); xlabel('Time (seconds)');
set(get(ax(1),'Ylabel'),'String','Compliance (mL/mmHg)');
set(get(ax(2),'Ylabel'),'String','Pressure (mmHg)');
set(h1,'LineStyle','-','LineWidth',1.5);
set(h2,'LineStyle','--','LineWidth',1.5);
xlim(ax(1),[0,t(r)]);
xlim(ax(2),[0,t(r)]);
hold off;

%-------------------------------------------------------------------------
%-------------------------------------------------------------------------

function PlotComparisonCvsP(c,h,v,cwave,hwave,vwave)

% Plots Pressure vs. Compliance for all data sets

x = figure('name','Pressure vs. Compliance
Comparison','numbertitle','off');
hold on;
plot(c(:,1),cwave,'-k','LineWidth',1.5);
plot(c(1,1),cwave(1),'>','MarkerSize',8,'MarkerFaceColor','k', ...
      'MarkerEdgeColor','k');
plot(h(:,1),hwave,'-r','LineWidth',1.5);
plot(h(1,1),hwave(1),'>','MarkerSize',8,'MarkerFaceColor','r', ...
      'MarkerEdgeColor','r');
plot(v(:,1),vwave,'-b','LineWidth',1.5);
plot(v(1,1),vwave(1),'>','MarkerSize',8,'MarkerFaceColor','b', ...
      'MarkerEdgeColor','b');
%ylim([2.5,2.75]);
%xlim([60,160]);
title('Compliance-Pressure Loops'); xlabel('Pressure (mmHg)'); ...
      ylabel('Compliance (mL/mmHg)');
%legend('Control','Hypertensive','Vasodilated');
hold off;

%-------------------------------------------------------------------------
%-------------------------------------------------------------------------

function PlotComparisonCvsPI(c,i,cwave,iwave)

% Plots Pressure vs. Compliance for all data sets

x = figure('name','Pressure vs. Compliance
Comparison','numbertitle','off');
hold on;
plot(c(:,1),cwave,'-k','LineWidth',1.5);
plot(c(1,1),cwave(1),'>','MarkerSize',8,'MarkerFaceColor','k', ...
```

```
      'MarkerEdgeColor','k');
plot(i(:,1),iwave,'-m','LineWidth',1.5);
plot(i(1,1),iwave(1),'>','MarkerSize',8,'MarkerFaceColor','m', ...
      'MarkerEdgeColor','k');
title('Pressure vs. Compliance Loops'); xlabel('Pressure (mmHg)'); ...
      ylabel('Compliance (mL/mmHg)');
%legend('Control','Ischemia');
hold off;

%-------------------------------------------------------------------------
%-------------------------------------------------------------------------

function P = CalcP(d,C,Z)

% Calculate Pressure from Q, Rs, C
% d = data set
% c = compliance (independent of P)

dt = 0.01;  % sampling interval (10 msec)
Rs = mean(d(:,1)) / mean(d(:,2));   % Peripheral Resistance

Pt(1) = d(1,1);  % Initial Pressure (measured)
for x = 1:length(d(:,1))-1
    Pt(x+1) = Pt(x) + dt.*(d(x,2)-Pt(x)./Rs)./C;
end

P = d(:,2).*Z + Pt(:);  % Pressure

%-------------------------------------------------------------------------
%-------------------------------------------------------------------------

function P = CalcPd(d,C,Z)

% Calculate Pressure from Q, Rs, C(P)
% d = data set
% c = compliance (dependent of P)

dt = 0.01;  % sampling interval (10 msec)
Rs = mean(d(:,1)) / mean(d(:,2));   % Peripheral Resistance

Pt(1) = d(1,1);  % Initial Pressure (measured)
for x = 1:length(d(:,1))-1
    Pt(x+1) = Pt(x) + dt.*(d(x,2)-Pt(x)./Rs)./C(x);
end

P = d(:,2).*Z + Pt(:);  % Pressure

%-------------------------------------------------------------------------
%-------------------------------------------------------------------------

function PlotPredPressures(t,d,P,Pd,cat)

% Plot measured and calculated pressures
% t = time
% P = predicted Pressure (Pressure-independent C)
```

```
% Pd = predicted Pressure (Pressure-dependent C(P))

x = figure('name','Pressure Predictions','numbertitle','off');
hold on;
[r c] = size(d);
plot(t(1:r),d(:,1),'-k');    % Measured Pressure
plot(t(1:r),P,'--b');        % Predicted Pressure (C)
plot(t(1:r),Pd,'--r');        % Predicted Pressure (C(P))
title([cat]); xlabel('Time (seconds)'); ylabel('Pressure (mmHg)');
legend('Measured Pressure','Predicted Pressure (C)', ...
      'Predicted Pressure (C(P))');
end
```

REFERENCES

1. Bohr, D., Webb R. "Vascular smooth muscle function and its changes in hypertension." *American Journal of Medicine*. Vol. 77:4A, 1984, pp. 3-16.

2. Bonow R., Mann D., Zipes D., Libby P. Braunwald's Heart Disease: A Textbook of Cardiovascular Medicine 9th ed. Saunders Elseveir, 2011, chap. 43, 46.

3. Burattini R., Gnudi G. "Computer identification of models for the arterial tree input impedance: Comparison between two new simple models and first experimental results." *Medical and Biological Engineering and Computing*. Vol. 20:2, 1982, pp. 134-44.

4. Calonge N., Petitti D., DeWitt T., et al. "Aspirin for the prevention of cardiovascular disease: U.S. Preventative Services Task Force recommendation statement." *Annals of Internal Medicine*. Vol. 150:6, 2009, pp. 396-404.

5. Cokkinos D., Pantos C., Heusch G., Taegtmeyer H. Myocardial Ischemia: From Mechanisms to Therapeutic Potentials. Springer Science, 2006, pp. 11-3.

6. Dart R., et. al. Medical Toxicology 3rd ed. Lippincott Williams & Wilkins, 2004, pp. 552-3.

7. Fantin F., Mattocks A., Bulpitt C., Banya W., Rajkumar C. "Is augmentation index a good measure of vascular stiffness in the elderly?" *Age and Ageing*. Vol. 36, 2007, pp. 43-8.

8. Frishman W., Cheng-Lai A., Nawarskas J. Current Cardiovascular Drugs 4th ed. Current Medicine LLC, 2005, pp. 265, 345.

9. Goldstein L., Bushnell C., et al. "Guidelines for the Primary Prevention of Stroke: A Guidelines for Healthcare Professionals From the American Heart Association/American Stroke Association." *Stroke: Journal of the American Heart Association*. Vol. 42, 2011, pp. 517-84.

10. Henrikson R., Kaye G., Mazurkiewicz J. National Medical Series: Histology. Lippincott Williams & Wilkins, 1997, pp. 173-4.

11. Jaffrin M. Biological Flows. Plenum Press, 1995, p. 237.

12. Li J K-J. Dynamics of the Vascular System. World Scientific Publishing Co. Pte. Ltd., 2004, pp. 130-141.

13. Li J K-J., Cui T., Drzewiecki G. "A Nonlinear Model of the Arterial System Incorporating a Pressure-Dependent Compliance." *IEEE Transactions on Biomedical Engineering*. Vol. 37:7, 1990, pp. 673-8.

14. Li J K-J., Zhu Y., Geipel P. "Pulse Pressure, Arterial Compliance and Wave Reflection Under Differential Vasoactive and Mechanical Loading." *Cardiovascular Engineering*. Vol. 10, 2010, pp. 170-5.

15. Lloyd-Jones D., Adams R., Carnethon M. "Heart Disease and Stroke Statistics – 2009 Update. A Report From the American Heart Association Statistics Committee and Stroke Statistics Subcommittee." *Circulation: Journal of the American Heart Association*. Vol. 119, 2009, pp. e1-e161.

16. Matonick J., Li J K-J. "Pressure-Dependent and Frequency Domain Characteristics of the Systemic Arterial System." *Cardiovascular Engineering*. Vol. 1:1, 2001, pp. 21-9.

17. McEniery C., Yasmin., Hall I., Qasem A., Wilkinson I., Cockcroft J. "Normal Vascular Aging: Differential Effects on Wave Reflection and Aortic Pulse Wave Velocity: The Anglo-Cardiff Collaborative Trial (ACCT)." *Journal of the American College of Cardiology*. Vol. 46:9, 2005, pp. 1753-60.

18. Murgo J., Westerhof N., Giolma J., Altobelli S. "Aortic input impedance in normal man: relationship to pressure wave forms." *Circulation: Journal of the American Heart Association*. Vol. 62, 1980, pp. 105-16.

19. National Research Council. Scientific and Humane Issues in the Use of Random Source Dogs and Cats in Research. The National Academies Press, 2009, pp. 49-50.

20. Nürnberger J., Keflioglu-Scheiber A., Saez A., Wenzel R., Philipp T., Schäfers R. "Augmentation index is associated with cardiovascular risk." *Journal of Hypertension*. Vol 20, 2002, pp. 2407-14.

21. O'Rourke M., Avolio A., Safar M., Nichols W. "Changes in the Central Pressure Pulse With Aging." *Journal of the American College of Cardiology*. Vol. 55:19, 2010.

22. Qureshi G., Brown R., Salciccioli L., Qureshi M., Rizvi S., Farhan S., Lazar J. "Relationship between aortic atherosclerosis and non-invasive measures of arterial stiffness." *Atherosclerosis*. Vol. 195:2, 2007, pp. e190-4.

23. Raff H. Physiology Secrets 2nd ed. Hanley & Belfus, Inc., 2003, p. 77.

24. Rhoades R., Bell D. Medical Physiology: Principles for Clinical Medicine 4th ed. Lippincott Williams & Wilkins, 2013, pp. 217-8.

25. Saba P., Roman M., Pini R., Spitzer M., Ganau A., Devereux R. "Relation of arterial pressure waveform to left ventricular and carotid anatomy in normotensive subjects." *Journal of the American College of Cardiology*. Vol. 22: 7, 1993, pp. 1873-80.

26. Sagawa K., Lie R., Schaefer J. "Translation of Otto frank's paper 'Die Grundform des arteriellen Pulses' zeitschrift für biologie 37: 483-526 (1899)." *Journal of Molecular and Cellular Cardiology*. Vol. 22:3, 1990, pp. 253-4.

27. Sasajima T., Bhattacharya V., Wu M., Shi Q., Hayashida N., Sauvage L. "Morphology and Histology of Human and Canine Internal Thoracic Arteries." *Annals of Thoracic Surgery*. Vol. 68, 1999, pp. 143-8.

28. Segars P., Georgakopoulos D., Afanasyeva M., et. al. "Conductance catheter-based assessment of arterial input impedance, arterial function, and ventricular-vascular interaction in mice." *American Journal of Physiology: Heart and Circulatory Physiology*. Vol. 288:3, 2005, pp. H1157-64.

29. Segers P., Qasem A., De Backer T., Carlier S., Verdonck P. "Peripheral 'Oscillatory' Compliance Is Associated With Aortic Augmentation Index." *Journal of Hypertension*. Vol. 27, 2001, pp. 1434-9.

30. Sherwood, L. Human Physiology: From Cells to Systems, 7th ed. Brooks/Cole, Cengage Learning, 2010, pp. 303-4, 343-7.

31. Shimizu M., Kario K. "Role of augmentation index in hypertension." *Therapeutic Advances in Cardiovascular Disease*. Vol 2:25, 2008, pp. 25-35.

32. Smith S., Scarth E., Sasada M. Drugs in Anaesthesia and Intensive Care 4th ed. Oxford University Press, 2011, pp. 220, 332.

33. Sparks H., Rooke T. Essentials of Cardiovascular Physiology. University of Minnesota Press, 1987, pp. 95-98.

34. Stergiopulos N., Westerhof B., Westerhof N. "Total arterial inertance as the fourth element of the windkessel model." *American Journal of Physiology: Heart and Circulatory Physiology.* Vol. 276, 1999, pp. H81-8.

35. Westerhof, N., Elzinga G., Sipkema P. "An artifical arterial system for pumping hearts." *Journal of Applied Physiology*. Vol. 31:5, 1971, pp. 776-81.

36. Westerhof N., Lankhaar J., Westerhof B. "The arterial Windkessel." *Med Biol Eng Comput*. 2008.

37. Westerhof N., Stergiopulos N., Noble M. Snapshots of Hemodynamics: An Aid for Clinical Research and Graduate Education 2nd ed. Springer, 2010, pp. 173-82.